



HUMBOLDT-UNIVERSITÄT ZU BERLIN
MATHEMATISCH-NATURWISSENSCHAFTLICHE FAKULTÄT I
INSTITUT FÜR PHYSIK

Efficient computation of meson and four-quark correlation functions

MASTERARBEIT

eingereicht von

CHRISTIAN WIESE

geboren am 04. Februar 1987 in Hagen

Aufgabensteller: Prof. Michael Müller-Preussker

Zweitgutachter: Prof. Marc Wagner

Abgabedatum: 24.09.2012

Abstract

This work deals with the efficiency of different methods for computing correlation functions of bound states in twisted mass lattice QCD with $N_f = 2$ flavors of sea-quarks. In particular, the focus will be on pseudo-scalar and scalar meson correlators as well as correlation functions generated by a four-quark operator. The main part of this thesis will be the comparison of three methods used to compute the quark propagator, namely the point-source method, the stochastic-source method and the one-end trick. All possible combinations of three valence quark masses which corresponds to light, strange and charmed mesons will be studied. For the four-quark study, the focus of this work will be on four-quark operators with the same quantum numbers as the D_{s0}^* and $a_0(980)$ mesons. This work shows results for the connected part of their correlator as well as presents and compares methods to compute the singly disconnected part.

Zusammenfassung

In dieser Arbeit wird die Effektivität verschiedener Methoden für die Berechnung von Korrelationsfunktionen gebundener Zustände in „Twisted mass lattice QCD“ untersucht. Dies beinhaltet sowohl die Korrelationsfunktionen von pseudoskalaren und skalaren Mesonen als auch Korrelationsfunktionen die mit Vier-Quark-Operatoren berechnet werden. Ein Großteil dieser Arbeit beschäftigt sich mit dem Vergleich von drei Methoden, die zur Berechnung des Quark-Propagators verwendet werden: die Punkt-Quellen-Methode, die Stochastische-Quellen-Methode und der One-End-Trick. Es werden alle möglichen Kombinationen von drei Valenzquarkmassen untersucht, was Mesonen mit leichten, Strange- und Charm-Quarks entspricht. Für die Vier-Quark-Korrelatoren wird sich diese Arbeit auf Operatoren konzentrieren, die die gleichen Quantenzahlen wie die $D_{s_0}^*$ - und $a_0(980)$ - Mesonen haben. Es werden verbundene Korrelatoren berechnet und Methoden für die Berechnung von einfach unverbundenen Korrelatoren eingeführt und verglichen.

Contents

1	Introduction	3
2	Basic Principles	5
2.1	Twisted mass lattice QCD	5
2.2	Extracting masses on the lattice	6
2.3	Notation	7
3	The meson correlator	8
3.1	Construction of a meson correlator	8
3.2	Computation of a meson correlator	10
3.2.1	Point-source method	10
3.2.2	Standard stochastic-source method	11
3.2.3	Stochastic noise reduction: The one-end trick	13
3.3	Additional spectroscopy methods	14
3.3.1	Partially quenched setup	14
3.3.2	Gauge field and quark field smearing	15
3.3.3	Generalized eigenvalue problem	16
3.3.4	Using twisted mass symmetries	17
4	Results and Interpretation: Mesons correlators	19
4.1	Simulation Setup	19
4.2	Meson results	20
4.3	Noise-to-signal ratio for stochastic techniques	20
4.3.1	Standard stochastic-source method	26
4.3.2	One-end trick	28
4.4	Increase of noise-to-signal ratio over Δt	29
4.5	The magnitude of gauge noise	30
4.6	The consequence of spin dilution	32
4.7	Different smearing locations	34
5	The four-quark correlator	37
5.1	Construction of a four-quark correlator	37
5.2	Computation of a four-quark correlator	40
5.2.1	Computing the connected correlator	40
5.2.2	Computing the singly disconnected correlator	40
6	Results and Interpretation: Four-quark correlators	42
6.1	Simulation setup	42

6.2	Computational methods	42
6.2.1	Methods for the singly disconnected term	42
6.2.2	Comparison of stochastic methods	44
6.3	Four-quark study ($D_{s_0}^*$ sector)	44
6.4	Four-quark study ($a_0(980)$ sector)	44
6.4.1	The four-quark correlator ($a_0(980)$ sector)	45
6.4.2	The influence of symmetry breaking on four-quark correlators	45
7	Summary, Conclusion and Outlook	48
7.1	Summary & Conclusion	48
7.1.1	Meson study	48
7.1.2	Four-quark study	49
7.2	Outlook	49
8	Bibliography	51

1 Introduction

A meson is a bound state of one quark and one antiquark. In experiments, around 175 meson states have been discovered. In the theory, quark models (e.g. [1][2]) and lattice calculations (e.g. [3][4]) are able to compute the spectrum and predict further states in addition to the states measured in experiments. While pseudo-scalar and vector mesons are easy to identify in experiments, the identification of scalar states still remains to be a problem [5]. This is due to a large decay width of those states and also, one expects exotic states like glue-balls and multi-quark states to appear in this sector.

On the lattice, pseudo-scalar mesons are relatively easy to compute, due to low statistical fluctuations and are often used to set the scale [6] or tune mass parameters [7]. Scalar mesons and excited states in general are harder to compute, due to large statistical fluctuations. In twisted mass QCD, which is an $\mathcal{O}(a)$ improved action, and used in many projects of the European Twisted Mass Collaboration, including spectroscopy [7][8][9], an additional problem occurs: Because of the symmetry breaking of the action, the correlator of an excited state cannot be computed independently, because a mixing between excited states and ground states occurs.

However, the spectroscopy of scalar mesons on the lattice is an important issue, because in combination with the experiment it can give information about the nature of scalar mesons. For the D_{s0}^* state, for example, a significant discrepancy between lattice computations and the experiment has been observed [10]. This is one of the reasons why the D_{s0}^* and other scalar mesons, such as the $a_0(980)$, are presumed to have four-quark components. A four-quark state is a hypothetical bound state consisting of two quarks and two antiquarks. The fact that scalar mesons can have four-quark components is an additional reason why they are challenging to compute.

The spectrum of states excited by four-quark operators can be computed on the lattice, but due to the mixing with lighter states and the number of possible diagrams, these studies are difficult to perform. While early lattice studies were performed with static quarks [11], in recent studies with dynamical quarks only the connected diagrams for these states were considered [12].

When computing the meson or four-quark spectrum on given gauge field configurations, most of the computation time has to be invested in computing the quark propagator. Therefore, applying an efficient method to compute these propagators is an important issue. However, up to now, there are only a few quantitative studies of

different methods for the computation of propagators, e.g. in [13]. A major part of this work will be the examination of three basic methods to compute the propagator in meson correlation functions:

- Using point sources,
- Using stochastic sources [14] [15],
- Reduced stochastic sources (the one-end trick) [16] [17].

I study the spectrum of scalar and pseudo-scalar mesons and use different valence quark masses in order to examine light, strange and charmed mesons. In addition, the efficiency of other spectroscopy methods, such as spin dilution and local smearing techniques, will be studied. Besides a numerical comparison of these techniques, this work will try to qualitatively understand properties of some methods, for example the magnitude of the stochastic noise or the increase of the noise-to-signal ratio for large temporal separations.

For the spectrum of states excited by four-quark operators, I will study candidates which have two types of diagrams in the correlation function, namely connected diagrams, where all four propagators connect two different points in time as well as singly disconnected diagrams, where two propagators form closed loops. The focus of this work will be on the singly disconnected diagrams. One needs complicated methods to compute them and they are suspected to have large statistical fluctuations. I will present two possible methods to compute these diagrams and compare the results in order to find a preferable method. I will use this method to compute singly disconnected diagrams of the $a_0(980)$ and the $D_{s_0}^*$ four-quark operators and will compare the results to the correlators of the connected diagrams. Due to the observation of an unexpected mixing with significantly light states in the correlation function, the symmetries of the four-quark operator will be studied. I will show that the initial operator is not an optimal operator and will propose an improved operator which could avoid a mixing with very light mesonic states like the pion.

I would like to start in section two with giving a short introduction into lattice QCD and spectroscopy of bound states. Section three will deal with the construction and computation of meson correlators, followed by section four where results for meson correlators will be presented and studied. In the second part of this work, section five shows how a four-quark correlator is constructed and can be computed. In section six results for the four-quark correlators will be shown and discussed. Lastly, in section seven I will summarize my results and give an outlook over further possible studies.

2 Basic Principles

2.1 Twisted mass lattice QCD

This work will not give a detailed introduction into lattice QCD. Instead the basic equations will be listed and I will focus on the extraction of masses on the lattice. A proper introduction into lattice QCD can be found in [18].

In my work I used $N_f = 2$ gauge configurations generated by the European Twisted Mass Collaboration (ETMC), which have already been used for several hadron spectrum computations (e.g. in [8, 9, 19]). The gauge action is the tree-level Symanzik improved gauge action

$$S_G[U] = \frac{\beta}{3} \sum_x \left(b_0 \sum_{\mu < \nu} \{1 - \text{Re Tr}(U_{x,\mu,\nu}^{1 \times 1})\} + b_1 \sum_{\mu,\nu} \{1 - \text{Re Tr}(U_{x,\mu,\nu}^{1 \times 2})\} \right) \quad (2.1)$$

where $\beta = 6/g_0^2$, $b_1 = -1/12$ and $b_0 = 1 - 8b_1$. $U_{x,\mu,\nu}^{1 \times 1}$ is the plaquette term, $U_{x,\mu,\nu}^{1 \times 2}$ a rectangular Wilson loop. As the fermionic action I used the Wilson twisted mass action (cf. [20] and references therein)

$$S_F[\chi, \bar{\chi}, U] = a^4 \sum_x \bar{\chi} (D_W + m + i\mu\gamma_5\tau_3) \chi \quad (2.2)$$

with D_W , the Wilson-Dirac operator, defined as

$$D_W = \frac{\gamma_\mu}{2} (\nabla_\mu + \nabla_\mu^*) + \frac{ar}{2} \nabla_\mu \nabla_\mu^* \quad (2.3)$$

Here, ∇_μ and ∇_μ^* are the forward and backward covariant derivatives on the lattice.

$$\nabla_\mu \psi(x) = \frac{1}{a} (U(x, \mu) \psi(x + a\mu) - \psi(x)) \quad (2.4)$$

$$\nabla_\mu^* \psi(x) = \frac{1}{a} (\psi(x) - U^\dagger(x - a\mu, \mu) \psi(x - a\mu)) \quad (2.5)$$

For the computation I use the twisted mass formalism in order to achieve an $\mathcal{O}(a)$ improvement. Instead of single flavor quark fields this action uses mass degenerated flavor doublets χ . The operator in the physical basis $\psi = (\psi_u, \psi_d)$ can now be obtained by applying a twist rotation to the spinors in the twisted basis and vice versa. In the continuum this rotation is given as:

$$\psi = \exp(i\omega\gamma_5\tau_3/2) \chi, \quad \bar{\psi} = \bar{\chi} \exp(i\omega\gamma_5\tau_3/2) \quad (2.6)$$

χ and $\bar{\chi}$ are the spinors in the twisted basis, ψ and $\bar{\psi}$ in the physical basis. The τ 's are the Pauli matrices acting in flavor space.

The twist angle ω satisfies the relation:

$$\tan \omega = \frac{\mu^R}{m^R} \quad (2.7)$$

where μ^R and m^R are renormalized masses. At maximal twist, the twist angle is $\omega = \pi/2$.

2.2 Extracting masses on the lattice

On the lattice, expectation values of operators are computed via

$$\langle \Omega | \mathcal{O}(t_1) \mathcal{O}(t_0) | \Omega \rangle = \frac{1}{N} \int D\chi D\bar{\chi} DU \mathcal{O}(t_1) \mathcal{O}(t_0) e^{-S_E[\chi, \bar{\chi}, U]} \quad (2.8)$$

$$N = \int D\chi D\bar{\chi} DU e^{-S_E[\chi, \bar{\chi}, U]} \quad (2.9)$$

where $S_E[\chi, \bar{\chi}, U] = S_F[\chi, \bar{\chi}, U] + S_G[U]$ is the Euclidean action of the system.

After analytically integrating out the fermionic fields, the path integral only depends on the gauge fields U . The integral can now be computed numerically by using a hybrid Monte Carlo algorithm to generate representative sets of gauge field configurations. Expectation values of operators can then be computed as means of observables on these configurations.

Masses of eigenstates of the Hamiltonian can be extracted by computing a suitable two-point or so-called correlation function:

$$C(t_1) = \langle \Omega | \mathcal{O}(t_1) \mathcal{O}^\dagger(t_0) | \Omega \rangle = \sum_n |\langle n | \mathcal{O} | \Omega \rangle|^2 e^{-(E_n - E_\Omega) \Delta t}, \quad \Delta t = t_1 - t_0 \quad (2.10)$$

Here, $|\Omega\rangle$ represents the vacuum state and E_Ω represents the vacuum energy.

By taking the limit $\Delta t \rightarrow \infty$, only the sum with the smallest energy gap $E_n - E_\Omega$ will remain.

$$\lim_{\Delta t \rightarrow \infty} \langle \Omega | \mathcal{O}(t_1) \mathcal{O}^\dagger(t_0) | \Omega \rangle = |\langle 1 | \mathcal{O} | \Omega \rangle|^2 e^{-(E_1 - E_\Omega) \Delta t} \quad (2.11)$$

E_1 is the energy of lowest non-trivial state of the system. However, in spectroscopy one is interested in the energy gap $E_1 - E_\Omega$, which is the mass of this state, so subsequently I will denote it $\tilde{E}_1 = E_1 - E_\Omega$.

Now the so-called effective mass is introduced:

$$m_{eff} = \ln \frac{\langle \Omega | \mathcal{O}(t_1) \mathcal{O}^\dagger(t_0) | \Omega \rangle}{\langle \Omega | \mathcal{O}(t_1 + 1) \mathcal{O}^\dagger(t_0) | \Omega \rangle} = E_n - E_\Omega \quad (2.12)$$

For large Δt , the effective mass will converge to the mass of the ground state.

$$\lim_{\Delta t \rightarrow \infty} \ln \frac{\langle \Omega | \mathcal{O}(t_1) \mathcal{O}^\dagger(t_0) | \Omega \rangle}{\langle \Omega | \mathcal{O}(t_1 + 1) \mathcal{O}^\dagger(t_0) | \Omega \rangle} = \tilde{E}_1 \quad (2.13)$$

However, when computing the meson spectrum, this definition of the effective mass is only approximate. Due to the periodic boundary conditions in time, the meson can propagate forwards and backwards in time. Thus, the correlation function cannot be described by a single exponential function. Instead it has to be described by a sum of two exponential functions which here is a hyperbolic cosine.

Note that one will only find a non-vanishing correlation function if $\langle 1 | \mathcal{O} | \Omega \rangle \neq 0$, i.e. the states $\mathcal{O} | \Omega \rangle$ and $| 1 \rangle$ overlap. Thus, if a suitable operator \mathcal{O} can be found, one can extract the energy of the ground state, which has the same quantum number as the operator \mathcal{O} .

2.3 Notation

In this work I would like to stick to the following conventions: Color indices are denoted by lower indices $a, b, c \dots = 1, 2, 3$ and spin indices are denoted by lower Greek indices $\alpha, \beta, \gamma \dots = 1, \dots, 4$. Sometimes I will use a spin and color super index denoted by a lower capital index $A, B, C \dots = 1, \dots, 12$. I will only use these indices if they are necessary.

The quark flavor will be given as an upper index in brackets $(i), (j) \in \{l, s, c; +, -\}$. Here, the $+, -$ denotes the twisted mass sign of the quark, where $l+$ is the up and $l-$ the down quark. A flavor index with a tilde (\tilde{i}) denotes a switched twisted mass sign. Upper indices n and m denote the sample of random numbers when using stochastic sources.

If possible, I will only use one index for the space-time coordinate $(x_1) = (\mathbf{x}_1, t_1)$.

3 The meson correlator

3.1 Construction of a meson correlator

I would like to start by introducing a meson creation operator. This operator has to be gauge invariant and have conserved quantum numbers, e.g isospin, parity and angular momentum. Taking into account these conditions, one possibility to write down a meson creation operator is:

$$\mathcal{O}(x) = \bar{\psi}_{a,\alpha}^{(i)}(x)(\Gamma_1)_{\alpha\beta}\psi_{a,\beta}^{(j)}(x) = \text{Tr}_{c,s}(\bar{\psi}^{(i)}(x)(\Gamma_1)\psi^{(j)}(x)) \quad (3.1)$$

This operator is gauge invariant and has certain quantum numbers, which are defined by Γ_1 , a 4×4 matrix in Dirac space. In this work I chose $\Gamma_1 \in \{\gamma_5, \mathbb{1}\}$, i.e. reducing the spectrum to pseudo-scalar and scalar mesons and $(i), (j) \in \{l, s, c\}$, i.e. all possible combinations of up, down, strange and charm quarks.

However, the standard $N_f = 2$ twisted mass action which is used, has no strange and charm quarks. Thus, I choose the partially quenched approach (see section 3.3.1). This means a twisted mass sign for strange and charm spinors has to be defined, because the twisted mass action only works for mass degenerated flavor doublets. I can do so because in the continuum, these flavor breaking effects disappear. In my work I compute all possible combinations of twisted mass signs. For every choice of quark flavors there are four possible combinations $(++, +-, -+, --)$. They split into two groups, which cannot be related by symmetries (equal or different twisted mass sign).

In order to relate the operator in the physical basis to an operator in the twisted mass basis, which I use on the lattice, it must be converted. This happens by rotating it into the twisted mass basis. This rotation is given by Eq. (2.6).

With the relation $\exp(i\gamma_5\omega) = \cos(\omega) + i\sin(\omega)\gamma_5$ it is easy to show the following identities for the twist rotation of mesons:

$$\bar{\psi}^{(i)\pm}\gamma_5\psi^{(j)\mp} = \bar{\chi}^{(i)\pm}\gamma_5\chi^{(j)\mp}, \quad \bar{\psi}^{(i)\pm}\mathbb{1}\psi^{(j)\mp} = \bar{\chi}^{(i)\pm}\mathbb{1}\chi^{(j)\mp} \quad (3.2)$$

$$\bar{\psi}^{(i)\pm}\gamma_5\psi^{(j)\pm} = \pm i\bar{\chi}^{(i)\pm}\mathbb{1}\chi^{(j)\pm}, \quad \bar{\psi}^{(i)\pm}\mathbb{1}\psi^{(j)\pm} = \pm i\bar{\chi}^{(i)\pm}\gamma_5\chi^{(j)\pm} \quad (3.3)$$

Note that these relations are only correct in the continuum. On the lattice the twist angle is not exactly $\pi/2$ and so these relations are only approximate.

Additionally, due to the twisted mass action, in a single correlator parity plus and minus or different isospin states can mix. However, when applying the right methods, it is still possible to extract the masses of single states (cf. section 3.3.3).

A suitable correlation function for extracting meson masses is:

$$C(\Delta t, p = 0) = \left\langle \frac{1}{V} \sum_{\mathbf{x}_1, \mathbf{x}_0} \mathcal{O}(t_1, \mathbf{x}_1) \mathcal{O}(t_0, \mathbf{x}_0)^\dagger \right\rangle \quad (3.4)$$

$\langle \rangle$ is the integration over all gauge and fermionic fields. Here, $\sum_{\mathbf{x}_1}$ is used to obtain a momentum zero projection. $1/V \sum_{\mathbf{x}_0}$ is the average over the spatial volume, and not mandatory. However, it can be used to reduce the noise caused by statistical fluctuations of the gauge field¹.

After inserting the operators, the integration over $\chi \bar{\chi}$ can be performed by using their Grassmann properties. The result is the inverse of the Dirac matrix, which is defined as the quark propagator.

$$\chi_A(x_1) \bar{\chi}_B(x_0) \rightarrow (D^{-1})_{AB}(x_1, x_0) \quad (3.5)$$

The correlation function in terms of propagators is as follows:

$$C(\Delta t) = - \left\langle \frac{1}{V} \sum_{\mathbf{x}_1, \mathbf{x}_0} \text{Tr}_{c,s} \left(\gamma_0 \Gamma_2^\dagger \gamma_0 D^{-1(i)}(\mathbf{x}_0, t_0, \mathbf{x}_1, t_1) \Gamma_1 D^{-1(j)}(\mathbf{x}_1, t_1, \mathbf{x}_0, t_0) \right) \right\rangle \quad (3.6)$$

Here, the $\langle \rangle$ is the integration over all gauge fields, which approximates, when using a suitable Monte-Carlo method, the average over a large number of gauge field configurations.

In this correlation function, the two propagators point in opposite directions. However, for some of the techniques, it is mandatory that they propagate in the same direction, i.e. both have the same starting point. Hence I will use the γ_5 -Hermiticity of the action to swap start and endpoint of one propagator:

$$D^{-1}(x_1, x_0) = \tau_1 \gamma_5 (D^{-1}(x_0, x_1))^\dagger \gamma_5 \tau_1 \quad (3.7)$$

$$C(\Delta t) = - \left\langle \frac{1}{V} \sum_{\mathbf{x}_1, \mathbf{x}_0} \text{Tr}_{c,s} \left(\tilde{\Gamma}_2 D^{-1(i)}(x_0, x_1) \tilde{\Gamma}_1 (D^{-1(j)}(x_0, x_1))^\dagger \right) \right\rangle \quad (3.8)$$

¹From now on I would like to refer to the noise caused by the statistical fluctuations of the gauge field as gauge noise

Here $\tilde{\Gamma}_1 = \Gamma_1 \gamma_5$ and $\tilde{\Gamma}_2 = \gamma_5 \gamma_0 \Gamma_2^\dagger \gamma_0$ is used.

In principle this expression could be evaluated on the lattice in order to extract the meson masses. However, computing the exact quark propagator, i.e. inverting the complete Dirac matrix, demands too much computation time, especially for large lattices. In the next section I will introduce methods to circumvent this problem.

3.2 Computation of a meson correlator

Typically, most of the computation time for the meson correlator has to be invested into computing the quark propagator. In this section I would like to introduce methods to compute the propagators, which appear in the discussed correlation functions.

3.2.1 Point-source method

The quark propagator is given by the inverse of the Dirac matrix D . An ansatz to compute the propagator is solving the following equation for a given ξ .

$$D\phi = \xi \tag{3.9}$$

where ϕ is called the sink and ξ the source of the propagator. The standard way of solving this equation is to use point sources, i.e. placing a single 1 on one element of the source:

$$\xi_A(x_2)[x_0, C] = \delta(x_2, x_0)\delta(A, C) \tag{3.10}$$

Here the indices in squared brackets denote the placement of the source point. We then have to solve the linear equation:

$$D_{A,B}(x_2, x_1)\phi_B(x_1)[x_0, C] = \delta(x_2, x_0)\delta(A, C) \tag{3.11}$$

And will obtain the propagator by computing

$$D_{B,C}^{-1}(x_1, x_0) = \phi_B(x_1)[x_0, C] \tag{3.12}$$

Now it is important to note that if one wants to compute the full propagator, i.e. not lose any information stored on the gauge configuration, it is necessary to solve

the linear equation for all possible source points x_0 and C . In practice this is an impossible task, because then the number of inversions is $V \cdot T \cdot N_s \cdot N_c$. Where V is the spatial volume of the lattice, T the temporal extension of the lattice, N_s the number of spin and N_c the number of color indices.

The straight-forward solution to this problem is taking advantage of the translation invariance of observables on the lattice and invert the Dirac matrix with only one fixed source point. This is the so called one-to-all propagator.

Now one end of the propagator $D_{B,C}^{-1}(x_1, x_0) = \phi_B(x_1)[x_0, C]$ is fixed to a chosen x_0 and one has to perform only 12 separate inversions, one for each C , which is color and spin.

The advantage of this technique is that I gain a one-to-all propagator, which does not contain any additional noise. The method is straightforward and easy to implement. However, it is not possible to average over all source points in order to gain all the information stored on a gauge configuration and therewith reduce the gauge noise. Furthermore, there are correlators with propagators where the source as well as the sink point needs to be varied (see section 5.2.2 on disconnected correlators of four-quark states). For these correlators, the point-source method cannot be used.

When using the point-sources method to compute the meson spectrum the following correlation function is used:

$$C(\Delta t, p = 0) = \sum_{\mathbf{x}_1} \text{Tr}_c (\Gamma_{\alpha,\beta} (\phi_\gamma(x_1)[x_0, \beta])^\dagger \Gamma_{\gamma,\delta} \phi_\delta(x_1)[x_0, \alpha]) \quad (3.13)$$

3.2.2 Standard stochastic-source method

In order to obtain an all-to-all propagator to reduce the gauge noise, I will follow [14] and [15] and construct a source spinor ξ , which has stochastic entries on all spatial lattice points of one single time slice.

$$\xi_A^n(x_1) = \delta(t_1, t_0) (Z_4)_A^n(\mathbf{x}_1) \quad (3.14)$$

In my work I consider noise, which is based on random numbers chosen from four entries of the complex unitary circle, i.e. $Z_4 = Z_2 \times Z_2 \in \{1/\sqrt{2}, -1/\sqrt{2}, i/\sqrt{2}, -i/\sqrt{2}\}$.

Basically, it is possible to use other types of noise as long as the following condition is fulfilled:

$$\langle (\xi_A^n(x_0))^\dagger \xi_B^n(x_1) \rangle = \delta_{x_0, x_1} \delta_{A, B} \quad (3.15)$$

Here, $\langle \rangle$ means averaging an infinite number of samples.

Now a sink is generated by solving the equation:

$$D_{A, B}(x_2, x_1) \phi_B^n(x_1) = \xi_A^n(x_2) \quad (3.16)$$

$$\phi_B^n(x_1) = D_{B, A}^{-1}(x_1, x_2) \xi_A^n(x_2) \quad (3.17)$$

The quark propagator can now be computed via the spinors ϕ and ξ^\dagger :

$$\langle \phi_A^n(x_1) (\xi_B^n(x_2))^\dagger \rangle = D_{A, C}^{-1}(x_1, x_3) \langle \xi_C^n(x_3) (\xi_B^n(x_2))^\dagger \rangle \quad (3.18)$$

$$= D_{A, B}^{-1}(x_1, x_2) \quad (3.19)$$

For an infinite number of samples this is the unbiased quark propagator. In practice, one can only compute the propagator for a finite number of samples n, m . Therefore, there are additional terms that are called stochastic noise. When using stochastic techniques, there is always stochastic noise in addition to the gauge noise. However, in comparison to the point-source method the gauge noise is reduced, because it is possible to average over the spatial source points.

Note that one temporal end of the propagator is fixed to t_0 due to construction of the source. Different temporal separations Δt , as needed for a correlation function, can still be achieved by the variation of t_1 .

I am going to write down the expression which is used on the lattice and will show that it equals the meson correlator in Eq. (3.8). I will omit the Γ structure.

$$C(\Delta t, p = 0) = \left\langle \frac{1}{V} \sum_{\mathbf{x}_0, \mathbf{x}_1} (\phi_A^n(x_1) (\xi_B^n(x_0))^\dagger \xi_B^m(x_0) (\phi_A^m(x_1))^\dagger) \right\rangle \quad (3.20)$$

$$= \left\langle \frac{1}{V} \sum_{\mathbf{x}_0, \dots, \mathbf{x}_3} \left(D_{AC}^{-1}(x_1, x_2) \xi_C^n(x_2) (\xi_B^n(x_0))^\dagger \xi_B^m(x_0) (\xi_D^m(x_3))^\dagger (D_{DA}^{-1}(x_1, x_3))^\dagger \right) \right\rangle \quad (3.21)$$

$$\approx \frac{1}{V} \sum_{\mathbf{x}_0, 1} \text{Tr}_{c, s} \left(D^{-1}(x_1, x_0) (D^{-1}(x_1, x_0))^\dagger \right) \quad (3.22)$$

I want to refer to this method as the standard stochastic-source method.

3.2.3 Stochastic noise reduction: The one-end trick

As seen later, the standard stochastic-source method will not provide better results than the point-source method, because more stochastic noise is added than gauge noise reduced, by averaging over the spacial volume.

However, the noise-to-signal ratio of the standard stochastic-source method can be improved when applying the so-called one-end trick which was used in [16] and [17], for example. In Eq. (3.21) there are four stochastic sources in total, which contain the stochastic noise. For the special case of mesons where one quark is propagating forwards and one quark backwards, this number can be reduced to two sources. When using the same sample of random numbers for the sources of both propagators it is possible to analytically erase one pair of ξ .

This results in a correlation function where two sinks are multiplied:

$$C(\Delta t, p = 0) = \left\langle \frac{1}{V} \sum_{\mathbf{x}_1} \text{Tr}_c \left((\phi_\alpha^n(x_1))^\dagger \Gamma_{\alpha\beta} \phi_\beta^n(x_1) \right) \right\rangle \quad (3.23)$$

$$= \left\langle \frac{1}{V} \sum_{\mathbf{x}_{0\dots 2}} \left((\xi^n(x_0))^\dagger (D^{-1}(x_1, x_0))^\dagger \Gamma D^{-1}(x_1, x_2) \xi^n(x_2) \right) \right\rangle \quad (3.24)$$

$$\approx \frac{1}{V} \sum_{\mathbf{x}_{0,1}} \text{Tr}_{c,s} \left((D^{-1}(x_1, x_0))^\dagger \Gamma D^{-1}(x_1, x_0) \right) \quad (3.25)$$

This correlator only equals the meson correlation function Eq. (3.8) if $\Gamma_2 = \mathbf{1}$. In order to not be limited to this special case, one needs the concept of spin dilution for the stochastic sources. This means I reduce the noise not only to one single time slice but also one spin slice:

$$\begin{aligned} \xi_{\alpha,a}^n(x_2)[\beta] &= \delta_{t_2,t_0} \delta_{\alpha,\beta} (Z_4)_a^n(\mathbf{x}_2) \\ D_{A,B}(x_2, x_1) \phi_B^n(x_1)[\gamma] &= \xi_A^n(x_2)[\gamma] \\ \Rightarrow \phi_B^n(x_1)[\gamma] &= D_{B,A}^{-1}(x_2, x_1) \xi_A^n(x_2)[\gamma] \end{aligned} \quad (3.26)$$

Due to spin dilution, one has to invert four times for each gauge configuration and each sample n . The random numbers Z_4 are generated once and copied four times to each of the four spin slices. If the γ matrices that are used are diagonal, it might be helpful to use different random number for each spin slice, but if they are not diagonal, it is mandatory to use the same set of random numbers for each spin slice.

Using spin dilution, I can write down the meson correlation function for the one-end trick:

$$C(\Delta t, p = 0) = \left\langle \frac{1}{V} \sum_{\mathbf{x}_1} \text{Tr}_c \left(\Gamma_{\gamma, \delta} (\phi_\alpha^n(x_1)[\gamma])^\dagger \Gamma_{\alpha, \beta} \phi_\beta^n(x_1)[\delta] \right) \right\rangle \quad (3.27)$$

$$= \left\langle \frac{1}{V} \sum_{\mathbf{x}_0, \dots, \mathbf{x}_2} \left((\xi_\epsilon^n(x_2)[\gamma])^\dagger (D_{\epsilon\alpha}^{-1}(x_1, x_2))^\dagger \Gamma_{\alpha\beta} D_{\beta\eta}^{-1}(x_1, x_0) \xi_\eta^n(x_0)[\delta] \Gamma_{\delta, \gamma} \right) \right\rangle \quad (3.28)$$

$$\approx \frac{1}{V} \sum_{\mathbf{x}_0, \mathbf{x}_1} \text{Tr}_{c,s} \left((D^{-1}(x_1, x_0))^\dagger \Gamma_1 D^{-1}(x_1, x_0) \Gamma_2 \right) \quad (3.29)$$

The one-end trick has the shortest contraction time of all the methods I compared. The drawback is, of course, the necessity of four inversions for each gauge configuration, which will not reduce the error caused by the stochastic noise due to the same set of random numbers for each spin slice.

3.3 Additional spectroscopy methods

In addition to the estimation of quark propagators there are several additional computation techniques that are used when extracting the meson spectrum. I will present the most important ones very briefly.

3.3.1 Partially quenched setup

Because there are no strange and charm quarks as valence quarks in the $N_f = 2$ twisted mass action, one needs an alternative way to compute the propagator for these quarks. In this work I will choose the partially quenched method.

For the computation of the quark propagator, this means that an action with a different mass μ is used for strange and charm quarks.

$$D(\mu_{s/c})\phi = \xi \quad (3.30)$$

The $\mu_{s/c}$ has to be tuned using the masses of the kaon and the D meson, for example, as done in [7].

Note that using this setup with twisted mass QCD will provide a quark doublet for strange as well as charm quarks. These quarks are denoted by + or - signs and are

only equal in the continuum. In this work, I will study all possible twisted mass sign combinations. The discrepancy of results gained with a different twisted mass setup can provide information about the discretization effects.

Of course, this method only provides strange and charm valence quarks, corresponding sea quarks are still neglected.

3.3.2 Gauge field and quark field smearing

From section 2.2 it is known that the mass of a bound state can be computed by the two point function of a suitable operator:

$$C(\Delta t) = \langle \Omega | \mathcal{O}(t_1) \mathcal{O}^\dagger(t_2) | \Omega \rangle = \sum_n |\langle n | \mathcal{O} | \Omega \rangle|^2 e^{-(E_n - E_\Omega) \Delta t} \quad (3.31)$$

When interested in computing the energy of the state $E_1 - E_\Omega$, one has to go to large Δt in order to reduce contributions of excited states. In addition to that, one can create an operator which has little overlap with the excited states:

$$\langle n | \mathcal{O}_s | \Omega \rangle \ll \langle 1 | \mathcal{O}_s | \Omega \rangle \text{ for } n > 1 \quad (3.32)$$

This can reduce the contribution of excited states even for smaller Δt .

At this point I introduce the concept of smearing. Instead of creating a local operator, the quark field and gauge field smearing create an operator with spatial extension which has a better overlap to the ground state (cf. [8] and references therein). In the correlation function, this is achieved by smearing the contributing propagators, i.e. smearing the fermionic source and sink fields, and gauge fields.

A disadvantage of smearing the fields is that it increases the error of the correlator. However, this effect is compensated because when it is possible to fit a mass plateau for smaller temporal separations, the error of the mass decreases.

The fermionic fields were smeared using Gaussian smearing with the parameters $N_{Gauss} = 30$ and $\kappa_{Gauss} = 0.5$. The gauge fields were smeared using APE smearing with the parameters $N_{APE} = 30$ and $\kappa_{APE} = 0.5$.

For the one-end trick and point-source method there is an additional aspect which must be considered. The smearing operator acts on both sides of the quark propagator. For the standard stochastic-source method this means that one can apply

the smearing operator to the sinks and sources while contracting. For the one-end trick and the point-source method there are only sinks used in the contraction. This means that the sources have to be smeared before performing the inversion.

For the case of the one-end trick I will also study a smearing technique already applied for meson spectroscopy [23]. Here, the smearing operator acts only on one side of the propagator. This is supposed to reduce the overlap to excited states without an increase of the noise-to-signal ratio. Here, one can perform the smearing on the sink or the source side of the propagator.

For lattice calculations especially only smearing the sink is preferable, because un-smeared stochastic-source inversions are more universal than smeared ones. Additionally, only smearing the sink during the contraction saves computation time while computing the propagator. Only smearing the source will save just a small amount of computation time during the contraction.

For the noise-to-signal ratio it should analytically make no difference which side of the propagator is smeared, due to the symmetry of the correlator. However, when using stochastic methods it could make a difference, according to [23]. In this work both smearing location will be examined.

3.3.3 Generalized eigenvalue problem

When computing the correlation function for excited mesons, one will find a mixing of states in this correlators. This is due to parity and isospin breaking in the twisted mass formalism. In this work, one will find a mixing between parity plus and minus states in the correlator for the scalar meson.

Thus, instead of computing the correlation function independently, I will compute a correlation matrix, which is defined by the following expression:

$$\tilde{C}_{ij}(t) = \langle \Omega | \mathcal{O}_i(t) \mathcal{O}_j(0)^\dagger | \Omega \rangle \quad (3.33)$$

Here, the \mathcal{O}_i are different operators that might mix. From this matrix, the masses of the n lowest states can be extracted by solving the generalized eigenvalue problem [21], where n is the dimension of the correlation matrix.

$$\tilde{C}_{ij}(t) v_j^n(t, t_0) = \lambda^n(t, t_0) \tilde{C}_{ij}(t_0) v_j^n(t, t_0), \quad n = 1, \dots, N \quad t > t_0 \quad (3.34)$$

The effective masses are then computed as

$$m_n^{\text{eff}} = \frac{1}{a} \ln \frac{\lambda_n(t, t_0)}{\lambda_n(t+a, t_0)} \quad (3.35)$$

In the limit $t \rightarrow \infty$, these effective masses approach the n lowest masses in the corresponding sector. As before, the masses of the n states are obtained by fitting a mass plateau to the effective masses.

Due to the mixing of states it is not trivial which operator \mathcal{O}_i corresponds to the effective mass m_n^{eff} . However, it can be investigated by computing the eigenvectors $v_j^n(t, t_0)$.

When examining the squared absolute value of the eigenvector $|v_j|^2$, belonging to the effective mass n , one can identify the dominating creation operator \mathcal{O}_j by the largest value $|v_j|^2$. This only works if the operators have the same norm. This can be achieved by choosing a similar structure for the operator, which is done in this work. If this is not possible, the operators have to be normalized by the computation of trial states.

3.3.4 Using twisted mass symmetries

When doing spectroscopy of mesons, small statistical errors are mandatory. Therefore, it is helpful to compute all possible combinations of twisted mass signs of contributing quarks, all possible γ matrices, as well as both time directions, because most of these combinations are identical in the average. One can use the symmetries of the twisted mass action to find these relations and average over the correlation functions.

These symmetries for the twisted mass Dirac operator are as follows:

γ_5 hermiticity:

$$D^{-1}(x_1, x_2) = \tau_1 \gamma_5 \left(D^{-1}(x_2, x_1) \right)^\dagger \gamma_5 \tau_1 \quad (3.36)$$

time reversal

$$D^{-1}(t_1, t_2) = \tau_1 \gamma_0 \gamma_5 D^{-1}(-t_1, -t_2) \gamma_5 \gamma_0 \tau_1 \quad (3.37)$$

charge conjugation

$$D^{-1}(x_1, x_2) = \gamma_0 \gamma_2 \left(D^{-1}(x_2, x_1) \right)^T \gamma_2 \gamma_0 \quad (3.38)$$

parity

$$D^{-1}(x_1, x_2) = \tau_1 \gamma_0 D^{-1}(-\mathbf{x}_2, -\mathbf{x}_1) \gamma_0 \tau_1 \quad (3.39)$$

Some of these symmetries ensure a hermitian correlation matrix, the others can be use to lower the statistical error of the computation. As an example I will apply time reversal to the correlation function of the D meson, with two positive twisted mass quarks.

$$\begin{aligned} C(t)(D_s, u+, c+) &= \\ &= \left\langle \frac{1}{V} \sum_{\mathbf{x}_1, \mathbf{x}_2} \text{Tr}_{c,s} \left(\gamma_5 D^{-1u+}(\mathbf{x}_2, t_2, \mathbf{x}_1, t_1) \gamma_5 D^{-1c+}(\mathbf{x}_1, t_1, \mathbf{x}_2, t_2) \right) \right\rangle \\ &= \left\langle \frac{1}{V} \sum_{\mathbf{x}_1, \mathbf{x}_2} \text{Tr}_{c,s} \left(\gamma_5 \gamma_0 \gamma_5 D^{-1u-}(\mathbf{x}_2, -t_2, \mathbf{x}_1, -t_1) \gamma_5 \gamma_0 \cdot \right. \right. \\ &\quad \left. \left. \cdot \gamma_5 \gamma_0 \gamma_5 D^{-1c-}(\mathbf{x}_1, -t_1, \mathbf{x}_2, -t_2) \gamma_5 \gamma_0 \right) \right\rangle \\ &= \left\langle \frac{1}{V} \sum_{\mathbf{x}_1, \mathbf{x}_2} \text{Tr}_{c,s} \left(\gamma_5 D^{-1u-}(\mathbf{x}_2, -t_2, \mathbf{x}_1, -t_1) \gamma_5 D^{-1c-}(\mathbf{x}_1, -t_1, \mathbf{x}_2, -t_2) \right) \right\rangle \\ &= C(-t)(D_s, u-, c-) \end{aligned} \quad (3.40)$$

One gains the correlation function of the D meson in negative time direction with two negative twisted mass quarks.

method	point	stochastic	one-end
# inversions / conf	$12 \cdot N_f$	$12 \cdot N_f$	$4 \cdot N_f$
# configurations	20	20	60
\approx norm. contr. time	1	24	0.5

Table 1: information about the number of inversions for each gauge configuration, the number of gauge configurations and the contraction time for all three methods of my meson spectroscopy study. The normalized contraction time is the contraction time divided by the contraction time of the point-source method

4 Results and Interpretation: Mesons correlators

4.1 Simulation Setup

The contractions and inversions in this work were done using $(L/a)^3 \times T/a = 24^3 \times 48$ lattice gauge field configurations. These configurations were generated at $\beta = 3.9$, corresponding to a lattice spacing of $a = 0.079(2)$ fm [6].

For the light quarks I used a valence and sea quark mass of $\mu = 0.0040$, which corresponds to a pion mass of $m_\pi = 336$ MeV. For strange and charm quark I used the partially quenched approach with valence quark masses of $\mu_c = 0.26$ and $\mu_s = 0.022$, which correspond to physical K and D meson masses [7].

Details on how many gauge configurations and inversions were used can be found in Table 1. The numbers were chosen so that the computational costs for each technique were equal. However, I neglected the contraction time and therefore will also list it in the mentioned table. It has to be noted that neglecting the contraction time is reasonable when using light quarks, because the cost of computing one propagator is a factor of two to three larger in comparison to the point-source contraction. However, the cost of computing a strange quark propagator is only a factor of 0.25 and computing the charm quark even a factor of 0.05. Thus, for contractions where only charm and strange propagators are used, the contraction time contributes strongly to the overall computation time.

4.2 Meson results

The first results that will be presented in Figure 1 are two exemplary effective masses for the pion and the D_s meson and their parity partners, using the three discussed techniques. From these plots one will be able to estimate the statistical error, which can be expected from the numbers of gauge configurations I used. To compare the different techniques one could now simply compare the errors of the effective masses. However, this will not be done in this work.

Instead, the error of the correlation functions will be examined, because they are a fundamental observable which is easily accessible. Furthermore, they have a simple structure, which can be investigated by analytical models. Due to better comparison, I will present the relative error or noise-to-signal ratio of the correlator $\Delta C/C$, which is the error of the correlator divided by its absolute value.

I computed all possible combinations of quark flavors, the pseudo-scalar and scalar meson and equal and different twisted mass sign for the two quarks, which amounts to a total number of 72 correlation functions which I present in Figures 2, 3, 4 and 5.

These plots can now be used to decide which methods is suitable for a certain meson computation. After examining the results a few points can be made.

- Most important, for meson computations the one-end trick should be preferred to the standard stochastic-source method. For every single correlation function the one-end trick provides a better noise-to-signal ratio.
- For light mesons and excited states the one-end trick provides results of better quality than the point-source method. This means that these are states with a relatively large gauge noise.
- For all other mesons both methods provides results of equal quality.

4.3 Noise-to-signal ratio for stochastic techniques

The presented results suggest that the one-end trick is by a factor of three to five better than the standard stochastic-source method. I will try to explain this factor with analytical methods. The noise-to-signal ratio or relative error of the correlator $\Delta C/C$ can be evaluated as follows.

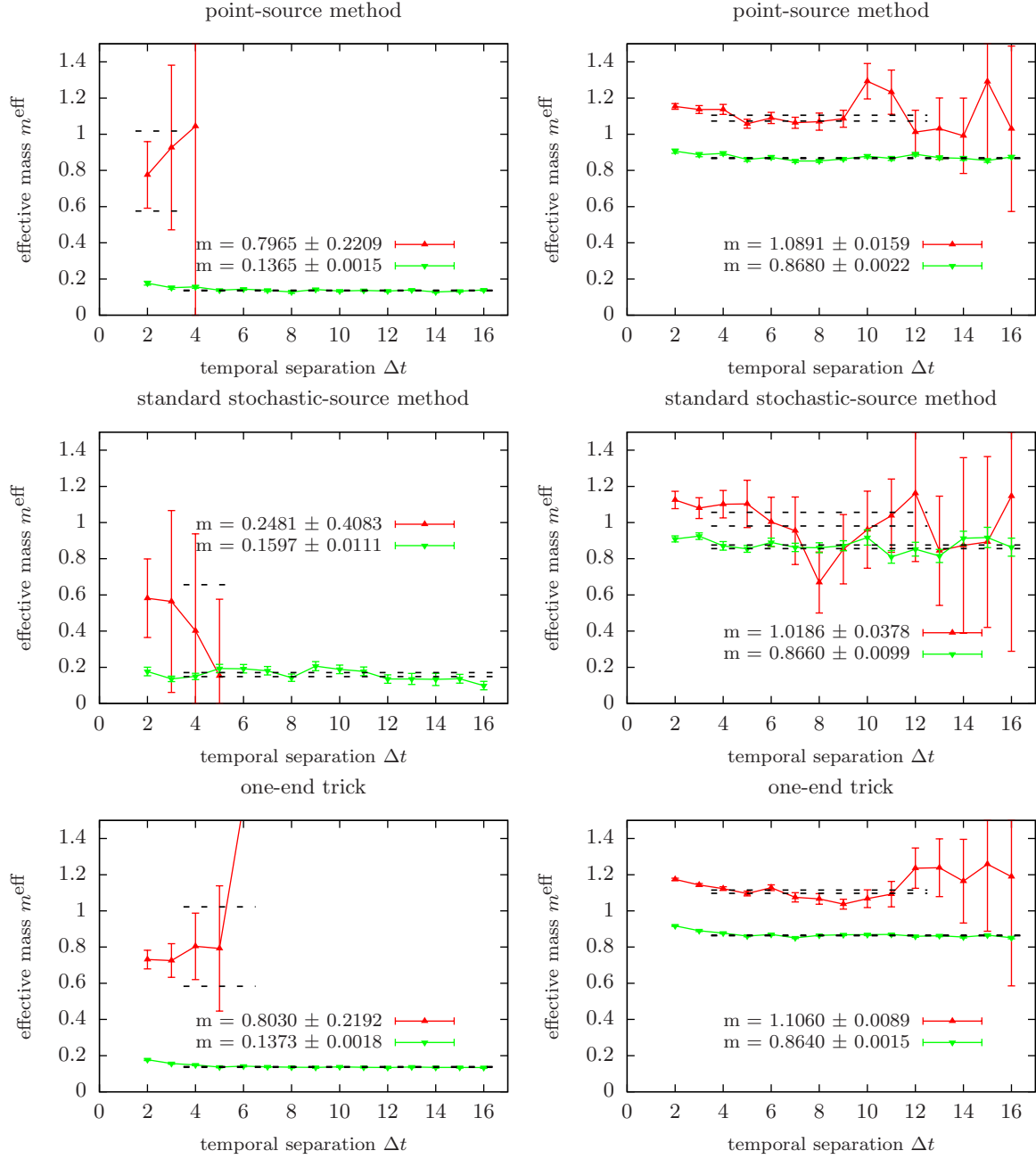


Figure 1: effective masses for the light-light (left) and the strange-charm (right) meson sectors for three different methods: point-source method (top), standard stochastic-source method (middle) and one-end trick (bottom); the upper plateau corresponds to scalar mesons, lower plateau to pseudo-scalar mesons.

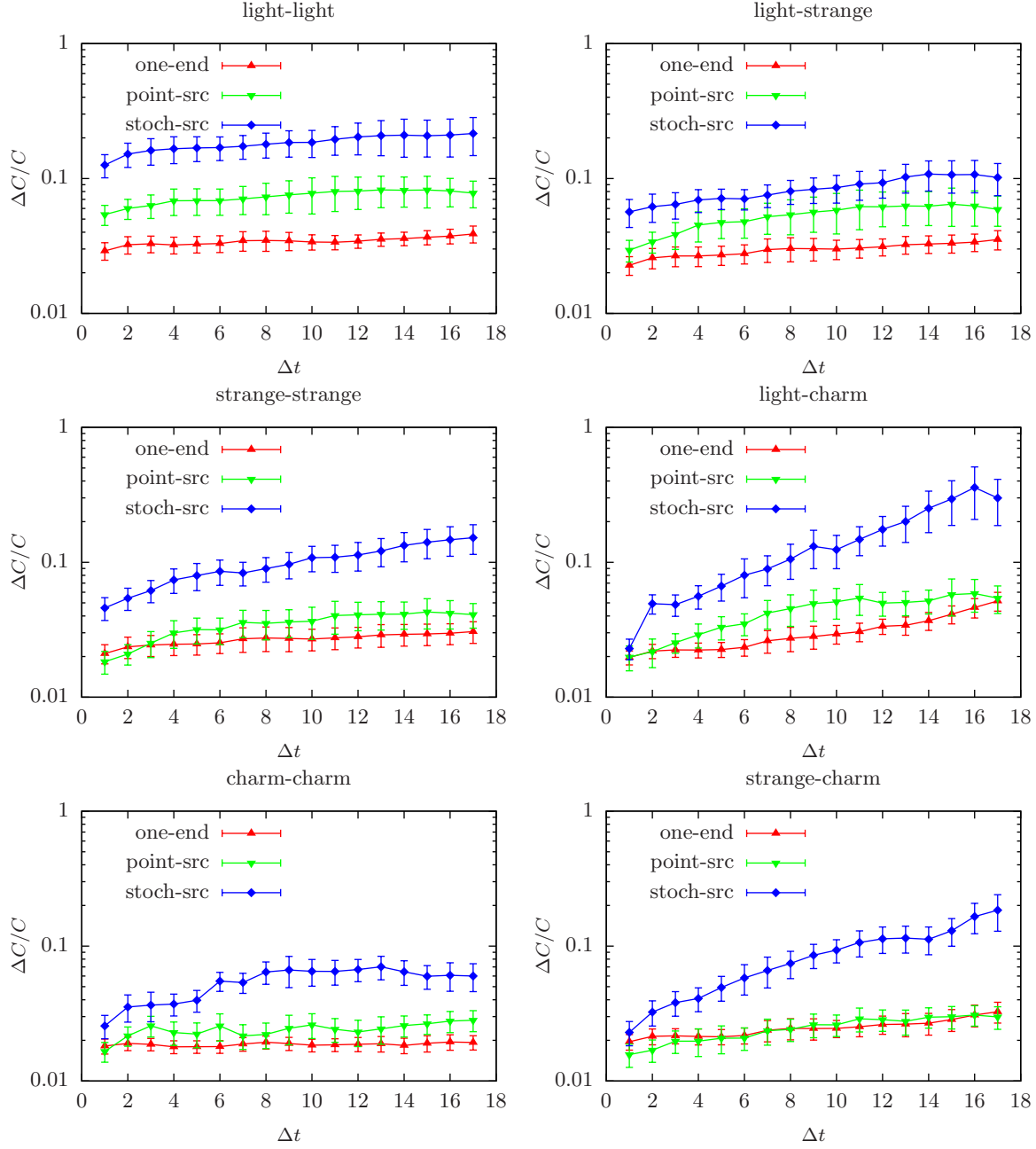


Figure 2: noise-to-signal ratio for all possible pseudo-scalar meson correlators using quarks with different twisted mass signs (e.g. $\mathcal{O} = \bar{\phi}^+ \gamma_5 \phi^-$); the three methods used are point-source method, standard stochastic-source method and the one-end trick.

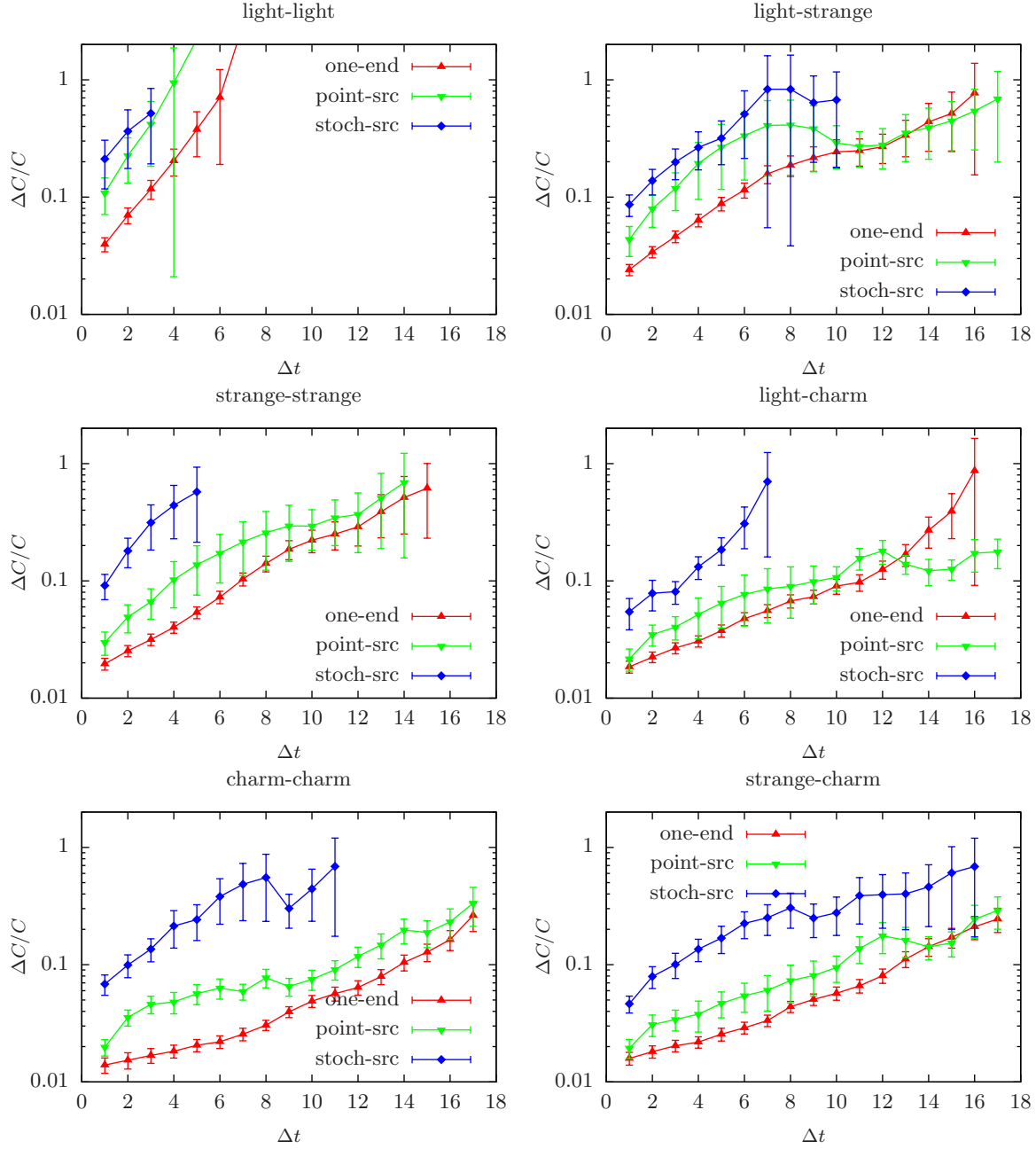


Figure 3: noise-to-signal ratio for all possible scalar meson correlators using quarks with different twisted mass signs (e.g. $\mathcal{O} = \bar{\phi}^+ \mathbb{1} \phi^-$); the three methods used are point-source method, standard stochastic-source method and the one-end trick.

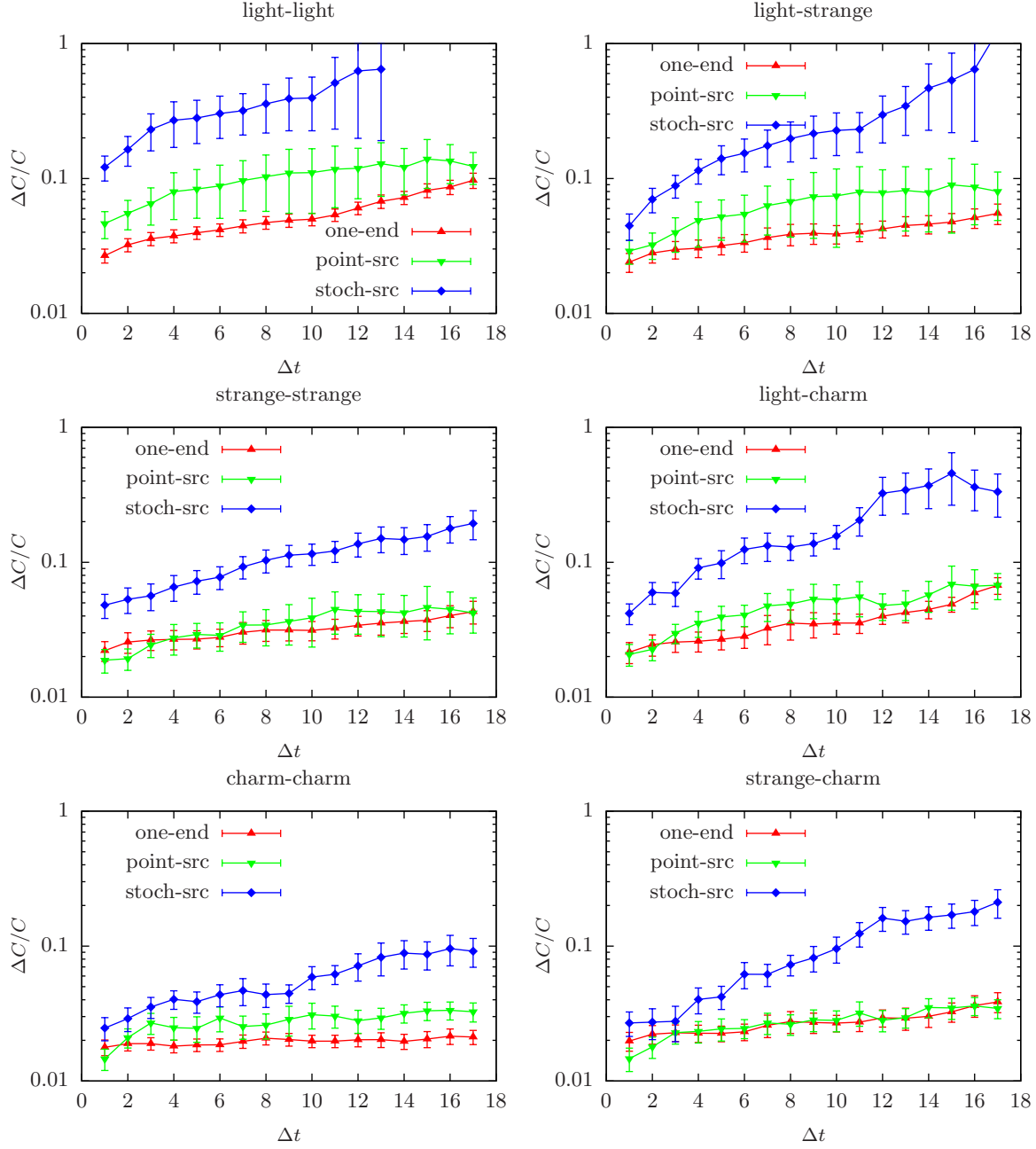


Figure 4: noise-to-signal ratio for all possible pseudo-scalar meson correlators using quarks with equal twisted mass signs (e.g. $\mathcal{O} = \bar{\phi}^+ \gamma_5 \phi^+$); the three methods used are point-source method, standard stochastic-source method and the one-end trick.

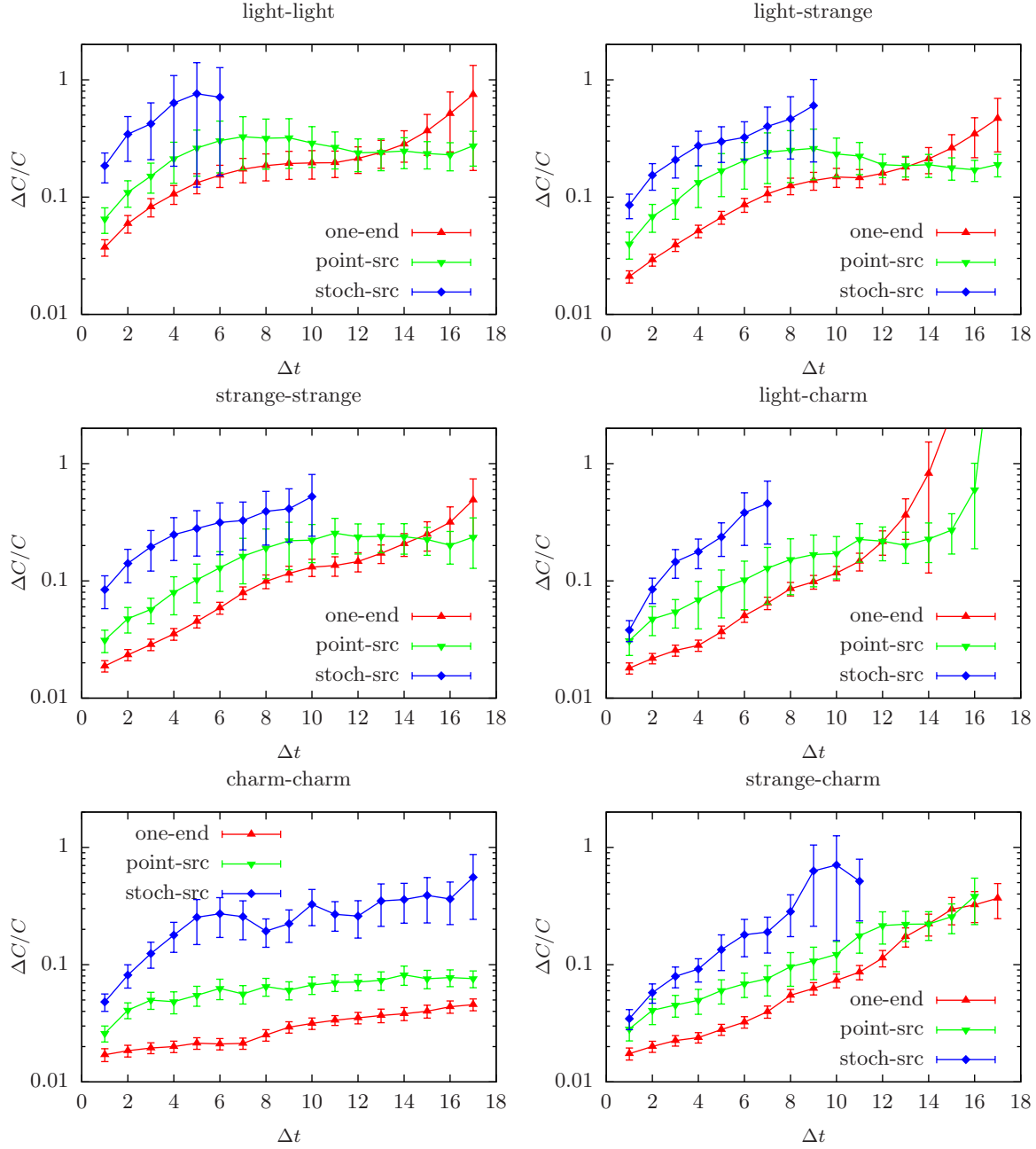


Figure 5: noise-to-signal ratio for all possible scalar meson correlators using quarks with equal twisted mass signs (e.g. $\mathcal{O} = \bar{\phi}^+ \mathbb{1} \phi^+$); the three methods used are point-source method, standard stochastic-source method and the one-end trick.

The error of the correlator is given by:

$$\Delta C = \frac{1}{\sqrt{N_0}} \sqrt{\langle |C|^2 \rangle - \langle C \rangle^2} \quad (4.1)$$

Here N_0 is the number of gauge field configurations. The relative error I am interested in computes as:

$$\frac{\Delta C}{C} = \frac{1}{\sqrt{N_0}} \sqrt{\frac{\langle |C|^2 \rangle - \langle C \rangle^2}{\langle C \rangle^2}} = \frac{1}{\sqrt{N_0}} \sqrt{\frac{\langle |C|^2 \rangle}{\langle C \rangle^2} - 1} \quad (4.2)$$

4.3.1 Standard stochastic-source method

In practice, it is not possible to evaluate $\langle |C|^2 \rangle$ and $\langle C \rangle$, due to the quark propagators appearing in the correlation function. Thus, I would like to use a simple model where I set all elements of the propagator, i.e. all signal terms, equal one, so that only the stochastic sources remain.

The equation for the correlator with all the contributing stochastic sources is as given in Eq. (3.21):

$$\begin{aligned} \langle C \rangle &= \\ &= \frac{1}{V} \frac{1}{N_1^2} \sum_{n,m} \sum_{\mathbf{x}_1 \dots \mathbf{x}_4} \left(D^{-1}(x_1, x_3) \xi^n(x_3) (\xi^n(x_2))^\dagger \xi^m(x_2) (\xi^m(x_4))^\dagger (D^{-1}(x_1, x_4))^\dagger \right) \end{aligned} \quad (4.3)$$

$$= \frac{1}{V} \frac{1}{N_1^2} \sum_{n,m} \sum_{\mathbf{x}_2 \dots \mathbf{x}_4} \sum_{B,C,D} (\xi_C^n(x_3) (\xi_B^n(x_2))^\dagger \xi_B^m(x_2) (\xi_D^m(x_4))^\dagger) \quad (4.4)$$

$$= \frac{1}{V} \frac{1}{N_1^2} (N_1^2 N_c N_s V) = N_c N_s \quad (4.5)$$

Here N_1 is the number of stochastic samples for the standard stochastic-source method. In the last line there is the factor $N_c N_s V N_1^2$ from the summation over all sources. Due to the construction of ξ one will only get a signal for $\mathbf{x}_2 = \mathbf{x}_3 = \mathbf{x}_4$, which is a factor V , $B = C = D$, which gives a factor $N_c N_s$ and a factor N^2 from the summation over the samples.

For estimating the noise-to-signal ratio, the expectation value of $|C|^2$ is also needed:

$$\begin{aligned}
\langle |C|^2 \rangle &= \langle CC^\dagger \rangle \\
&= \frac{1}{V^2} \frac{1}{N_1^4} \sum_{\mathbf{x}_{2\dots 4}} \sum_{B,C,D} \sum_{\tilde{\mathbf{x}}_{2\dots 4}} \sum_{\tilde{B},\tilde{C},\tilde{D}} \sum_{n,m} \sum_{\tilde{n},\tilde{m}} \\
&\quad (\xi_C^n(x_3)(\xi_B^n(x_2))^\dagger \xi_B^m(x_2)(\xi_D^m(x_4))^\dagger \xi_D^{\tilde{m}}(\tilde{x}_4)(\xi_{\tilde{B}}^{\tilde{m}}(\tilde{x}_2))^\dagger \xi_{\tilde{B}}^{\tilde{n}}(\tilde{x}_2)(\xi_{\tilde{C}}^{\tilde{n}}(\tilde{x}_3))^\dagger) \quad (4.6)
\end{aligned}$$

The following terms appear due to the summation over the sources:

$$\begin{aligned}
&N_1^2 V^3 N_c^3 N_s^3 \text{ when } \mathbf{x}_3 = \tilde{\mathbf{x}}_3, \mathbf{x}_2 = \tilde{\mathbf{x}}_2, \mathbf{x}_4 = \tilde{\mathbf{x}}_4, \\
&\quad A = \tilde{A}, B = \tilde{B}, C = \tilde{C}, n = \tilde{n}, m = \tilde{m} \\
&N_1^4 V^2 N_c^2 N_s^2 \text{ when } \mathbf{x}_2 = \mathbf{x}_3 = \mathbf{x}_4, \tilde{\mathbf{x}}_2 = \tilde{\mathbf{x}}_3 = \tilde{\mathbf{x}}_4, \\
&\quad B = C = D, \tilde{B} = \tilde{C} = \tilde{D} \\
&-N_1^2 V N_c N_s \text{ when } \mathbf{x}_2 = \mathbf{x}_3 = \mathbf{x}_4 = \tilde{\mathbf{x}}_2 = \tilde{\mathbf{x}}_3 = \tilde{\mathbf{x}}_4, \\
&\quad B = C = D = \tilde{B} = \tilde{C} = \tilde{D}, n = \tilde{n}, m = \tilde{m}
\end{aligned}$$

The last term is appearing twice in the other terms and thus has to be subtracted.

The relative error one finds for the standard stochastic-source method is then:

$$\frac{\Delta C}{C} = \frac{1}{\sqrt{N_0}} \sqrt{\frac{V N_c N_s}{N_1^2} - \frac{1}{V N_c N_s N_1^2} + 1} - 1 \quad (4.7)$$

$$= \frac{1}{N_1 \sqrt{N_0}} \sqrt{V N_c N_s - \frac{1}{V N_c N_s}} \approx_{(V \gg 1)} \frac{1}{N_1 \sqrt{N_0}} \sqrt{N_c N_s V} \quad (4.8)$$

In order to be able to directly compare this result to the one-end trick I will perform the same computation for the one-end trick.

4.3.2 One-end trick

For the one-end trick I find the following expectation value of the correlator starting from Eq. (3.28):

$$\langle C \rangle = \frac{1}{V} \frac{1}{N_2} \sum_n \sum_{\mathbf{x}_{1\dots 3}} \left((\xi^n[\beta](x_3))^\dagger (D^{-1}(x_1, x_3))^\dagger D^{-1}(x_1, x_2) \xi^n[\alpha](x_2) \right) \quad (4.9)$$

$$= \frac{1}{V} \frac{1}{N_2} \sum_n \sum_{\mathbf{x}_{2,3}} \text{Tr}_{c,s} \left((\xi^n[\beta](x_3))^\dagger \xi^n[\alpha](x_2) \right) \quad (4.10)$$

$$= \frac{1}{V} \frac{1}{N_2} (N N_c V) = N_c \quad (4.11)$$

Here N_2 is the number of stochastic samples for the one-end trick. The factor V is from $\mathbf{x}_2 = \mathbf{x}_3$ and N_2 from summation over the samples. In contrast to the standard stochastic-source method, I only find a factor N_c instead of $N_c N_s$ due to spin dilution. For the one-end trick the expectation value of $|C|^2$ is:

$$\begin{aligned} \langle |C|^2 \rangle &= \frac{1}{V^2} \frac{1}{N_2^2} \sum_{\mathbf{x}_{2\dots 3}} \sum_{B,C} \sum_{n,\tilde{n}} \sum_{\tilde{\mathbf{x}}_{2\dots 3}} \sum_{\tilde{B},\tilde{C}} \\ &\quad (\xi_B^n[\alpha](x_2) (\xi_C^n[\beta](x_3))^\dagger (\xi_{\tilde{B}}^{\tilde{n}}[\alpha](\tilde{x}_2))^\dagger \xi_{\tilde{C}}^{\tilde{n}}[\beta](\tilde{x}_3)) \end{aligned} \quad (4.12)$$

From the sources one finds the following terms:

$$\begin{aligned} &N_2^2 V^2 N_c^2 \text{ when } \mathbf{x}_2 = \mathbf{x}_3, \tilde{\mathbf{x}}_2 = \tilde{\mathbf{x}}_3, B = C, \tilde{B} = \tilde{C} \\ &N_2 V^2 N_c^2 \text{ when } \mathbf{x}_2 = \tilde{\mathbf{x}}_2, \mathbf{x}_3 = \tilde{\mathbf{x}}_3, B = \tilde{B}, C = \tilde{C}, n = \tilde{n} \\ &-N_2 V N_c \text{ when } \mathbf{x}_2 = \tilde{\mathbf{x}}_2 = \mathbf{x}_3 = \tilde{\mathbf{x}}_3, B = \tilde{B} = C = \tilde{C}, n = \tilde{n} \end{aligned}$$

Again, the last term is appearing twice. The noise-to-signal ratio is as follows:

$$\frac{\Delta C}{C} = \frac{1}{\sqrt{N_0}} \sqrt{\frac{1}{N_2} + 1 - \frac{1}{V N_c N_2}} - 1 \quad (4.13)$$

$$= \frac{1}{\sqrt{N_0}} \sqrt{\frac{1}{N_2} - \frac{1}{V N_c N_2}} \approx_{(V \gg 1)} \frac{1}{\sqrt{N_2 N_0}} \quad (4.14)$$

For the one-end trick I only used one sample for each gauge configuration, so here $N_2 = 1$. When now comparing this result with the standard stochastic-source method I gain the following relation between the standard stochastic-source method and the one-end trick.

$$\frac{\Delta C / C_{stoch.}}{\Delta C / C_{oneend}} = \sqrt{\frac{(N_0)_{stoch.}}{(N_0)_{oneend}}} \frac{1}{N_1} \sqrt{N_c N_s V} \quad (4.15)$$

Here, N_1 is the number of samples for the standard stochastic-source method. If I insert $N_1 = 12$ and consider a factor of three more gauge configurations for the one-end trick I gain an analytic factor of around 100. However, in the numerical data one finds a factor of three to five.

This suggests that the noise-to-signal ratio is dominated by the gauge noise, not by the stochastic noise. This is because the measured noise is caused by the statistical fluctuations of the gauge field and the noise from the stochastic sources, while in the model only the noise from the sources is considered.

However, then the one-end trick should provide results that are significantly better than the results gained by the point-source method, because the one-end trick reduces the statistical fluctuations of the gauge field. One does not find such a large difference.

Most possible, this discrepancy between the factors might simply come from using the simple model which replaces the propagators. They drop off exponentially for larger temporal and spatial separations and thus suppress certain contributions to the noise.

Nevertheless, both the numerical data and the model calculation support that the one-end trick should be the method of choice when it comes to computing meson correlation functions.

4.4 Increase of noise-to-signal ratio over Δt

For most of the correlation functions I observe an increase of the noise-to-signal ratio over Δt . I will try to explain this increase by a model and estimate the slope by using lattice data. The noise-to-signal ratio of a correlator is given by:

$$\left\langle \frac{\Delta C}{C} \right\rangle = \frac{1}{\sqrt{N_0}} \frac{\sqrt{\langle |C|^2 \rangle - \langle C \rangle^2}}{\langle C \rangle} = \frac{1}{\sqrt{N_0}} \sqrt{\frac{\langle C^2 \rangle}{\langle C \rangle^2} - 1} \quad (4.16)$$

The correlator $\langle C \rangle$ decreases with $\exp(-m_H t)$ for large Δt , where m_H is the mass of the computed hadron. That implies $\langle C \rangle^2 \sim \exp(-2m_H t)$. However, $\langle |C|^2 \rangle$ decreases with $\exp(-M_H t)$ where M_H is the mass of the lightest bound state with the same quantum numbers as two times the computed meson. This is usually a two-particle state.

When using this in Eq. (4.16), I find the following for the noise-to-signal ratio:

$$\langle \Delta C/C \rangle = \sqrt{\exp(-M_H \Delta t) / \exp(-2m_H \Delta t) - 1} \quad (4.17)$$

$$= \sqrt{\exp((2m_H - M_H)\Delta t) - 1} \quad (4.18)$$

$$\approx_{\Delta t \gg 1} \exp\left(\frac{1}{2}(2m_H - M_H)\Delta t\right) \quad (4.19)$$

As an example I would like to examine the error of the D meson and its parity partner the D_0^* meson.

As input masses I would like to use the lattice computations for these hadrons I performed on the given lattices: $am_D = 0.8264$, $am_{D_0^*} = 1.0636$. The lightest two-particle state with the same quantum numbers is a charmonium pion system: $aM_H = am_{PS} + am_{\eta_c} = 0.137 + 1.279 = 1.416$. Here the η_c is a pseudo-scalar meson with two charm quarks, where the disconnected diagram was neglected.

Thus, the relative error should show the following time dependence for the D_0^* :

$$\left\langle \frac{\Delta C}{C} \right\rangle_{D_0^*} = \exp\left(\frac{1}{2}(2m_{D_0^*} - m_{PS} - m_{\eta_c}) \cdot \Delta t\right) \quad (4.20)$$

$$\text{in lattice units} \approx \exp(0.3556 \cdot \Delta t) \quad (4.21)$$

The appearing multiplicative factors were neglected because I am only interested in the exponential slope. The same calculation can be done for the D meson:

$$\langle \Delta C/C \rangle(D) = \exp\left(\frac{1}{2}(2m_D - m_{PS} - m_{\eta_c}) \cdot \Delta t\right) \quad (4.22)$$

$$\text{in lattice units} \approx \exp(0.1184 \cdot \Delta t) \quad (4.23)$$

In Figure 6 I compare the numerical data of the one-end trick and the point-source method to my model calculation from above. For the function I used the calculated exponential slope and chose the multiplicative factor so that the function fitted the data. One can observe that this model provides an approximate estimation of the exponential slope of the error for excited states as well as ground states. One has to keep in mind that this estimation only holds for large temporal separations.

4.5 The magnitude of gauge noise

As already stated, I observed that for heavy mesons the stochastic methods, in comparison to the point-source method, are not so effective anymore as they are for

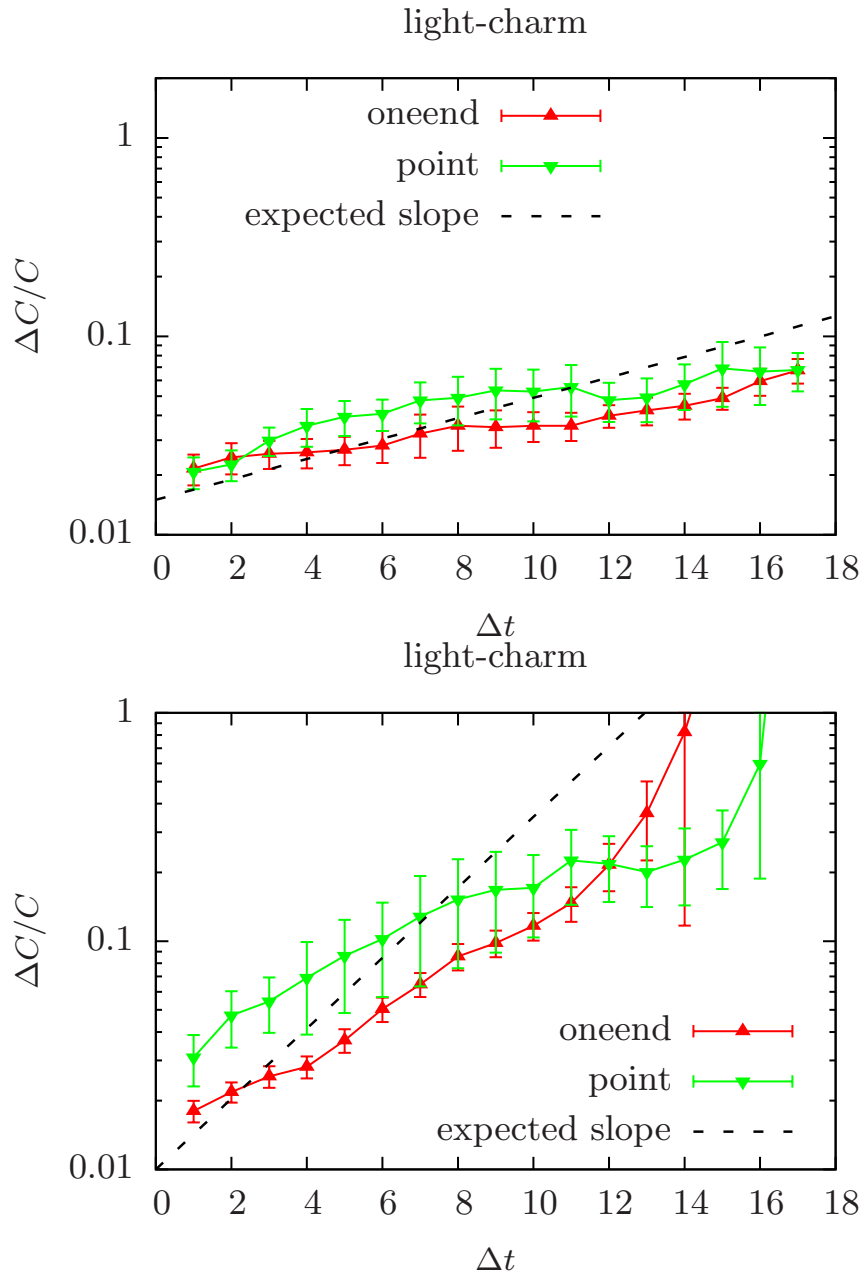


Figure 6: noise-to-signal ratio of the D meson (top) and the D_0^* meson (bottom) using one-end trick and point-source method in comparison to the estimated slope from Eq. (4.23) (top) and Eq. (4.21) (bottom)

light mesons. This suggests that for larger quark masses the ratio between gauge noise and stochastic noise decreases, while for lower quark masses the gauge noise is large in comparison to the stochastic noise.

The decrease of gauge noise for larger quark masses can be understood when looking at the Dirac operator:

$$D(x, y) = \frac{1}{2a} \gamma_\mu (U(x, \mu) \delta_{x, y - a\mu} - U^\dagger(x - a\mu, \mu) \delta_{x, y + a\mu}) + m_0 \delta_{x, y} \quad (4.24)$$

The mesonic correlation function only depends on the quark propagators which are the inverse of this operator.

It is obvious that for larger quark masses, i.e. a larger m_0 , the kinetic term, which contains the link variables, becomes small in comparison to the mass term. This means that for larger quark masses the gauge noise, which originates in the link variables, is suppressed.

However, the noise of the stochastic methods is not strongly effected by the quark mass. Thus, for heavier quark masses the error of the stochastic techniques will not decrease as fast as the error of the point-source method.

From the data I also observe an advantage of the one-end trick over the point-source method for the scalar mesons. This suggests that for scalar mesons the gauge noise is larger than for pseudo-scalar mesons.

4.6 The consequence of spin dilution

Especially for the heavy mesons, I observe a different exponential slope over Δt for the standard stochastic-source method and the one-end trick. However, the analytic model suggests that there is a constant factor between the methods. One possible assumption is that the advantage of spin dilution only shows up for large temporal separations, because at small distances there is no coupling between different spin components of the propagator, which would add noise to the system. This can be tested with performing a computation with the one-end trick without spin dilution, which only works for $\Gamma = \mathbb{1}$, i.e. all pseudo-scalar mesons when using quarks with different twisted mass signs, and comparing it to the standard one-end trick computations.

From the results shown in Figure 7 one can conclude the the following.

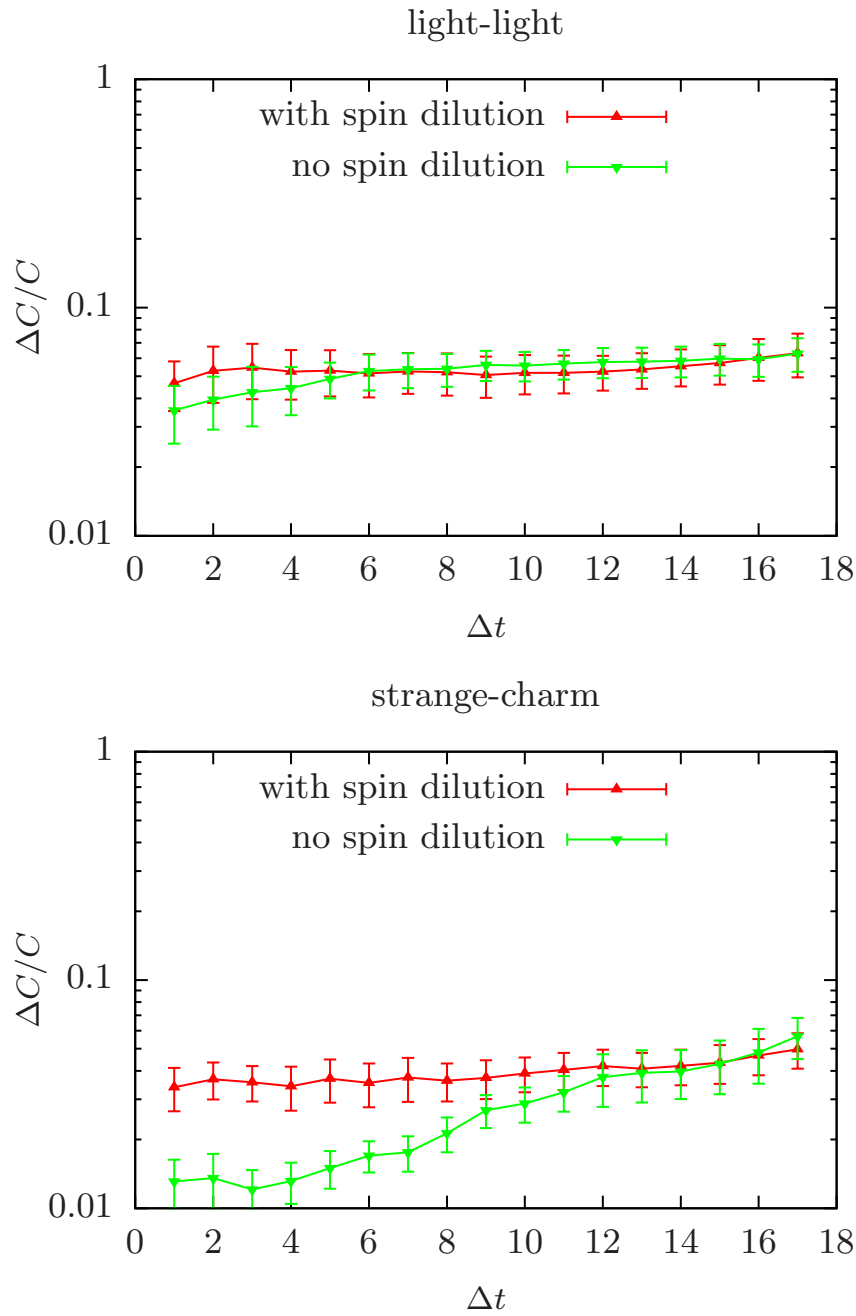


Figure 7: noise-to-signal ratio for the pion (top) and the D_s meson (bottom) using the one-end trick with and without spin dilution. For the two graphs the computational costs are not equal due to four inversions for spin dilution and only one inversion for no spin dilution

- I observe, especially for heavy mesons, a significant slope when not using spin dilution. This suggests that the noise from off-diagonal spin elements will only occur for larger temporal separations.
- However, I find an equal or even better noise-to-signal ratio for computational costs that are four times lower than for the ordinary one-end trick. This suggests that whenever it is possible to apply the one-end trick without spin dilution, one should do so.

For the D_s meson one observes a better noise-to-signal ratio for small temporal separations when using no spin dilution. At first this seems unusual, because one uses only one inversion instead of four. The reason for this is the different use of random numbers in the sources. While using spin dilution demands the same set of random numbers for each spin slice, the method with no spin dilution demands different random numbers. This means that when the spin dilution itself provides no advantage there is an additional positive effect when not using spin dilution due to the different random numbers on each spin slice.

4.7 Different smearing locations

To study the effect of different smearing techniques, three different meson correlators were computed, namely where both sink and source were smeared (smeared-smeared), where only the source was smeared (local-smeared) and where only the sink was smeared (smeared-local). The computations were done with 20 gauge field configurations and the one-end trick was used. I will present the noise-to-signal ratios and the effective masses of the D meson and the pion.

It is important to know that when only using smearing on one side, a possible correlation matrix is not hermitian anymore. Thus, the generalized eigenvalue problem in its standard form cannot be used. Instead, for the computation of excited states an alternative method is needed, e.g. the fitting of exponential functions. Therefore, I will only apply this method on correlators of ground states, because here the influence of a mixing with excited states can be neglected.

From the results shown in Figure 8 I would like to conclude the following.

- When using one of the one-sided smearing methods the effective mass drops to its plateau as fast as when using smearing on both sides.

- For the pion, however, I do not see a lower noise-to-signal ratio for those techniques.
- For the D meson I observe a slightly better noise-to-signal ratio for the smeared-local correlator, however, when the plateau is reached, this discrepancy vanishes within errors.

The first point can be understood from Eq. (3.31). The purpose of smearing is that $|\langle n|\mathcal{O}_s|\Omega\rangle|^2$ is small in comparison to $|\langle 1|\mathcal{O}_s|\Omega\rangle|^2$ for $n > 1$. When applying one-sided smearing this factor is replaced by $\langle\Omega|\mathcal{O}_s|n\rangle\langle n|\mathcal{O}^\dagger|\Omega\rangle$. Thus, if $\langle\Omega|\mathcal{O}_s|n\rangle$ is small in comparison to $\langle\Omega|\mathcal{O}_s|1\rangle$ the new factor is also small and the contribution of excited states is suppressed.

To sum up, the one-sided smearing techniques do neither seem to clearly improve the noise-to-signal ratio, nor do they influence the mass plateau. However, one could apply these techniques to save computation time.

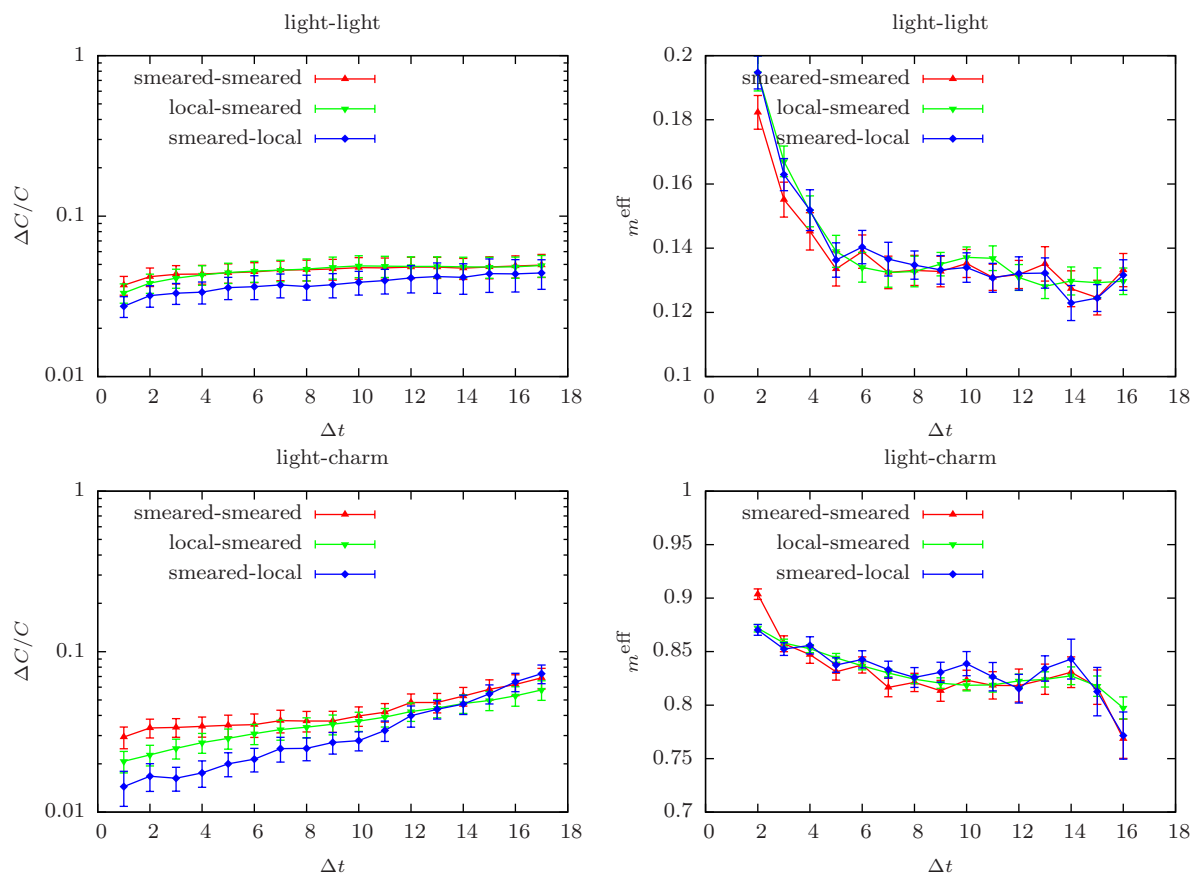


Figure 8: noise-to-signal ratios (left) and effective masses (right) for the pion (top) and the D meson (bottom) for the three mentioned smearing methods; notation: sink - source

5 The four-quark correlator

To understand the nature of scalar meson states, the study of four-quark correlation functions is an important issue. The comparison of quark models (cf. [24] and ref. therein) and lattice studies with the experiment suggest that besides the standard $q\bar{q}$ structure scalar mesons could have components of other quark or gluon structures. A natural candidate for this structure is a bound state of two mesons, due to the decay channel of scalar mesons into two mesons. This two meson structure of a four-quark operator will be studied here.

5.1 Construction of a four-quark correlator

In this work I would like to study two mesonic states which might have four-quark components. These are the $a_0(980)$ meson with the quantum numbers $I(J^P) = 1(0^+)$ and the $D_{s_0}^*$ meson with the quantum numbers $I(J^P) = 0(0^+)$ and $C = S = \pm 1$.

When writing down an operator for a four-quark state one has to note that there are two basic structures which can form a four-quark operator while being gauge invariant and having conserved quantum numbers. Here, I will refer to them as mesonic molecule and diquark-antidiquark. The differences between these structures are the contraction of color indices and spin indices. Here, I will briefly sketch the operator structure.

$$\mathcal{O}_{\text{mesonic}} = (\bar{\psi}_a \Gamma_1 \psi_a) (\bar{\psi}_b \Gamma_2 \psi_b) \quad (5.1)$$

$$\mathcal{O}_{\text{diquark}} = \epsilon_{abc} (\psi_b^T \Gamma_1 \psi_c) \epsilon_{ade} (\bar{\psi}_d^T \Gamma_2 \bar{\psi}_e) \quad (5.2)$$

In this work I will only study correlation functions from mesonic molecule operators. In order to create a bound state consisting of four quarks with $J^P = 0^+$ and $I = 1$ for the $a_0(980)$ candidate, I write down the following operator, which is the operator for the mesonic molecule. The decay mode of the $a_0(980)$ into $K\bar{K}$ suggests to use a strange quark and a strange antiquark for the two additional quarks.

$$\mathcal{O}_{a_0}(x) = \text{Tr}_{s,c} (\bar{\psi}_{s+}(x) \gamma_5 \psi_u(x)) \text{Tr}_{s,c} (\bar{\psi}_d(x) \gamma_5 \psi_{s+}(x)) \quad (5.3)$$

The mesonic molecule operator for the four-quark candidate $D_{s_0}^*$ has a similar structure. Additionally, there is a sum over the light quarks in order to obtain a light isospin of zero.

$$\begin{aligned} \mathcal{O}_{D_{s_0}^*}(x) = & \text{Tr}_{s,c}(\bar{\psi}_u(x)\gamma_5\psi_{s-}(x)) \text{Tr}_{s,c}(\bar{\psi}_u(x)\gamma_5\psi_{c-}(x)) + \\ & + \text{Tr}_{s,c}(\bar{\psi}_d(x)\gamma_5\psi_{s-}(x)) \text{Tr}_{s,c}(\bar{\psi}_d(x)\gamma_5\psi_{c-}(x)) \end{aligned} \quad (5.4)$$

In a very first step I will compare different methods to compute correlation function formed by four-quark operators. This means that I am not going to consider all possible twisted mass signs for the heavy quark but stick to one setup instead.

After rotating the operator in the twisted mass basis, the construction of the correlation function is now performed in the familiar way:

$$C(\Delta t, p = 0) = \sum_{\mathbf{x}_1} \langle \mathcal{O}(t_1, \mathbf{x}_1) \mathcal{O}(t_0, \mathbf{x}_0)^\dagger \rangle \quad (5.5)$$

Here, I drop the second sum immediately, because with none of the methods, I will present later on, it is possible to compute it.

However, an important feature appears when performing the Wick contractions. If two or more quark flavors of the four-quark operator are identical, there is more than one possibility to contract the spinors. For the operators I use, which have two identical quarks (u,d for the $D_{s_0}^*$; s for the $a_0(980)$), there are two ways to contract the spinors: The connected contraction, where each quark on time slice t_0 is contracted with its partner at time slice t_1 and the singly disconnected contraction, where on each time slice one pair of quarks on this single time slice is contracted. A schematic picture of these contraction is given in Figure 9, where each line represents a quark propagator.

I will start at this point with the expression for the connected part of the correlation function. When contracting quarks on different time slices I obtain a correlation function with four propagators, which all propagate between the same space time points forward or backward in time.

$$\begin{aligned} C_{\text{conn}}(\Delta t, p = 0) = & \left\langle \sum_{\mathbf{x}_1} \text{Tr}_{c,s}(\Gamma_1 D^{-1(i)}(x_1, x_0) \Gamma_2 D^{-1(j)}(x_0, x_1)) \cdot \right. \\ & \left. \cdot \text{Tr}_{c,s}(\Gamma_3 D^{-1(k)}(x_0, x_1) \Gamma_4 D^{-1(l)}(x_1, x_0)) \right\rangle \end{aligned} \quad (5.6)$$

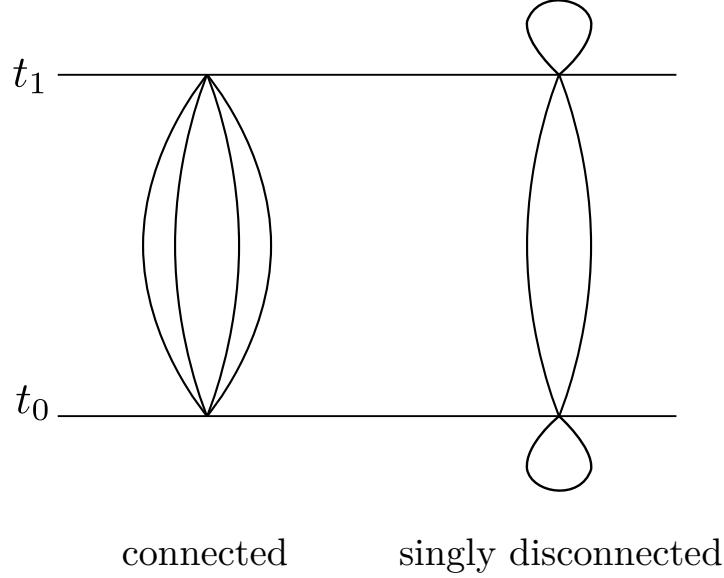


Figure 9: the two possible ways of Wick contractions for the $a_0(980)$ and the D_{s0}^* four-quark candidates

As for the mesons, I will use the γ_5 hermiticity of the action to let all quarks propagate in the same time direction.

$$C_{\text{conn}}(\Delta t, p = 0) = \left\langle \sum_{\mathbf{x}_1} \text{Tr}_{c,s} \left(\gamma_5 \Gamma_1 D^{-1(i)}(x_1, x_0) \Gamma_2 \gamma_5 \left(D^{-1(j)}(x_1, x_0) \right)^\dagger \right) \cdot \text{Tr}_{c,s} \left(\Gamma_3 \gamma_5 \left(D^{-1(\tilde{k})}(x_1, x_0) \right)^\dagger \gamma_5 \Gamma_4 D^{-1(l)}(x_1, x_0) \right) \right\rangle \quad (5.7)$$

This correlation function can be computed relatively easy on the lattice by using the point-source method to compute the quark propagator. I will introduce these computation methods in the next section.

For the disconnected terms, one finds an additional minus sign due to a different Wick contraction. The general structure of the singly disconnected propagator looks as follows:

$$C_{\text{disc}}(\Delta t, p = 0) = - \left\langle \sum_{\mathbf{x}_1} \text{Tr}_{c,s} \left(\Gamma_1 D^{-1(i)}(x_1, x_0) \Gamma_2 D^{-1(j)}(x_0, x_0) \Gamma_3 \gamma_5 \left(D^{-1(\tilde{k})}(x_1, x_0) \right)^\dagger \gamma_5 \Gamma_4 D^{-1(j)}(x_1, x_1) \right) \right\rangle \quad (5.8)$$

Unfortunately, this correlator is not easily computable, due to its structure. In the next section, I will explain the problem and introduce methods to solve it.

5.2 Computation of a four-quark correlator

5.2.1 Computing the connected correlator

For the connected part of the four-quark correlator it seems suitable to use the point-source method to compute the propagator. Using the stochastic-source method is not appropriate due to the large noise of the standard method and the fact that a one-end trick for four-quark correlators is not directly applicable. The standard one-end trick only works for two propagators having the same starting and endpoints.

When using the point-source method, the general structure of the correlator is as follows:

$$\begin{aligned}
C_{\text{conn}}(\Delta t, p = 0) &= \\
&= - \left\langle \sum_{x_2} \text{Tr}_c \left(\Gamma_{\alpha, \beta} (\phi_\gamma(x_1)[x_0, \beta])^\dagger \Gamma_{\gamma, \delta} \phi_\delta(x_1)[x_0, \alpha] \right) \right. \\
&\quad \left. \text{Tr}_c \left(\Gamma_{\alpha, \beta} (\phi_\gamma(x_1)[x_0, \beta])^\dagger \Gamma_{\gamma, \delta} \phi_\delta(x_1)[x_0, \alpha] \right) \right\rangle \quad (5.9)
\end{aligned}$$

This term can be easily computed on the lattice.

5.2.2 Computing the singly disconnected correlator

When trying to apply the same method for the disconnected term the following correlator will result:

$$\begin{aligned}
C_{\text{disc}}(\Delta t, p = 0) &= \\
&= - \left\langle \sum_{\mathbf{x}_0} \left(\phi_D(x_0)[A, x_1] \phi_A(x_1)[B, x_1] \right. \right. \\
&\quad \left. \left. (\phi_C(x_0)[B, x_1])^\dagger \phi_C(x_0)[x_0, D] \right) \right\rangle \quad (5.10)
\end{aligned}$$

Here, the term $\sum_{\mathbf{x}_0} \phi_C(x_0)[x_0, D]$ provides a significant problem. One would need an order of V inversions to gain all terms needed to compute the whole correlation

function. In practice this is not possible to carry out. The solution I chose is a mixed setup between point-source and stochastic-source inversions.

$$\begin{aligned}
C_{\text{disc}}(\Delta t, p = 0) &= \\
&= - \left\langle \sum_{\mathbf{x}_0} (\phi_D(x_0)[A, x_1] \phi_A(x_1)[B, x_1] \right. \\
&\quad \left. (\phi_C(x_0)[B, x_1])^\dagger \tilde{\phi}_C(x_0) (\tilde{\xi}_C(x_0))^\dagger \right\rangle \quad (5.11)
\end{aligned}$$

Here, the ϕ are sinks obtained the point-source method, while $\tilde{\phi}$ and $\tilde{\xi}$ are obtained by the stochastic-source method.

A problem that remains is the time dependence of the closed loop propagator at time t_1 . If t_0 is fixed, I need several values for t_1 , to find a dependence of the correlator on Δt . For this problem there are two possible solutions, which will presented here. One is choosing the stochastic entries on the source to be on the whole volume instead of being just on the spatial one, i.e. remove the restriction to a single time slice.

$$\tilde{\xi}_A^n(x) = (Z_4)_A^n(\mathbf{x}, t) \quad (5.12)$$

With this source we can access all time slices of the disconnected loop.

The other solution is keeping the noise restricted to one single time slice, but doing a larger number of inversions covering different time slices.

$$\tilde{\xi}_A^n(x) = \delta(t, t_0) (Z_4)_A^n(\mathbf{x}), \quad t_0 \in t_{\text{effm}} \quad (5.13)$$

Here t_{effm} are all the time points at which the effective mass needs to be studied. The number of inversions is determined by this number of points.

6 Results and Interpretation: Four-quark correlators

6.1 Simulation setup

For the computation of four-quark correlators I used the same gauge field configurations as for my meson computation. The following results were obtained on 20 gauge configurations. For the purpose of a initial test of the techniques this number is sufficient.

6.2 Computational methods

6.2.1 Methods for the singly disconnected term

As already mentioned, the four-quark correlators I am interested in split up in terms with two different structures. The study of computational methods will focus on the computation of the singly disconnected term (cf. section 5.1).

In section 5.2.2 I discussed two possible ways of computing the singly disconnected terms of the four-quark correlators. In order to determine the more efficient method I will study the comparison between stochastic entries on the whole volume and stochastic entries on one time slice for one of the singly disconnected terms in Figure 10. Again, I display the relative error of the correlator $\Delta C/C$, of the singly disconnected term with two up quark loops. For the stochastic volume noise I used 12 samples of stochastic sources for each gauge configuration. For the stochastic time-slice noise I used one sample for each gauge configuration, but the inversions were done for 6 different time slices. This number has to be chosen according to the number of time slices one is interested in.

Even if the error is very large, the plot suggests that using noise localised on a single time slice is a better choice for efficient computations. Thus, for the following computations of the singly disconnected terms I will use the stochastic time-slice noise method.

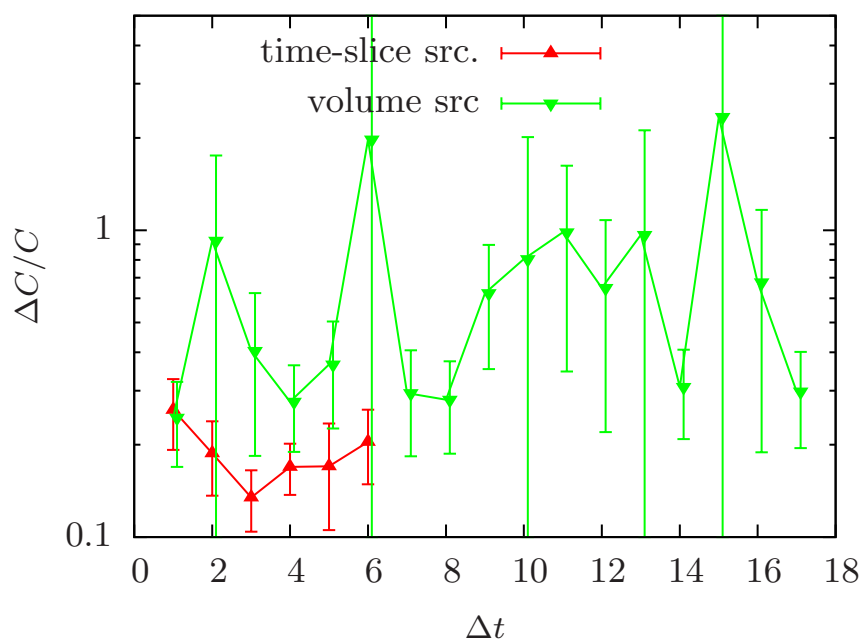


Figure 10: noise-to-signal ratio for stochastic entries on the volume and stochastic entries on one time slice for computing the singly disconnected terms of the four-quark correlator ($D_{s_0}^*$ sector)

6.2.2 Comparison of stochastic methods

Figure 10 suggests an approximate factor of two to three between the stochastic volume and the stochastic time-slice method. This factors can also be estimated by analytic arguments, when setting all signal terms of the propagator equal one.

When using stochastic entries on the whole volume, there are 48 more noise terms in comparison to stochastic entries on one time slice, due to the temporal extension of the lattice. This will increase the noise-to-signal ratio by a factor of $\sqrt{48}$ for the stochastic volume noise. However, for this technique I used 12 samples for each gauge configuration. This decreases the noise-to-signal ratio by a factor of $\sqrt{12}$. In total, this means that the stochastic time-slice noise is expected to be better than the stochastic volume noise by a factor of two. Note that this factor depends on the number of sources used for both methods and the number of time slices one is interested in.

6.3 Four-quark study (D_{s0}^* sector)

When using the four-quark operator (D_{s0}^* sector) in Eq. (5.4) in order to create a correlation function one will find a total number of six terms, two of which are connected and four of which are singly disconnected. In Fig. 11 I will show one of the singly disconnected terms (with two up quark loops) and the two connected terms in order to get an idea about how large the error of the singly disconnected term is in comparison to the connected one.

6.4 Four-quark study ($a_0(980)$ sector)

Due to the similar structure of the four-quark correlator of the $a_0(980)$ sector to the four-quark correlator of the D_{s0}^* sector I can reuse the contraction code from the former section for the $a_0(980)$ computations, with only changing the quark flavors and the Γ structure.

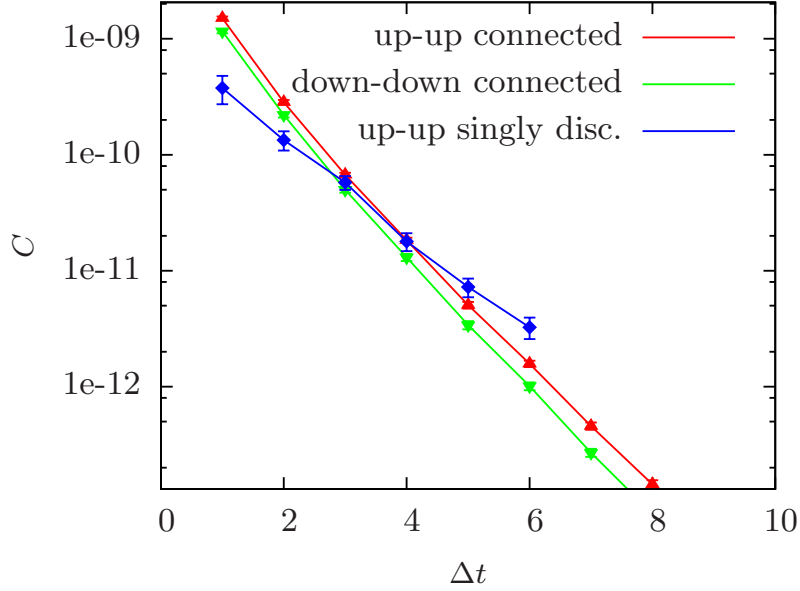


Figure 11: correlation function for both connected terms and one singly disconnected term of the four-quark correlator ($D_{s_0}^*$ sector). In the legend the flavors of the light propagators are denoted

6.4.1 The four-quark correlator ($a_0(980)$ sector)

When computing the four-quark correlator ($a_0(980)$ sector) from the operator in Eq. (5.3), there are only two terms, one connected and one singly disconnected. I present them in Figure 12.

For both terms I observe rather low statistical fluctuations. The slope of the singly disconnected term is very low and thus will dominate the correlation function after a few temporal separations. This is an important observation because it means that the singly disconnected term has a large influence on the correlator and cannot be neglected.

6.4.2 The influence of symmetry breaking on four-quark correlators

Figure 12 suggests that the singly disconnected term dominates the four-quark correlator ($a_0(980)$ sector) with a rather small slope, which, in turn, results in a small mass. Computing the effective mass of this disconnected term gives an approximate

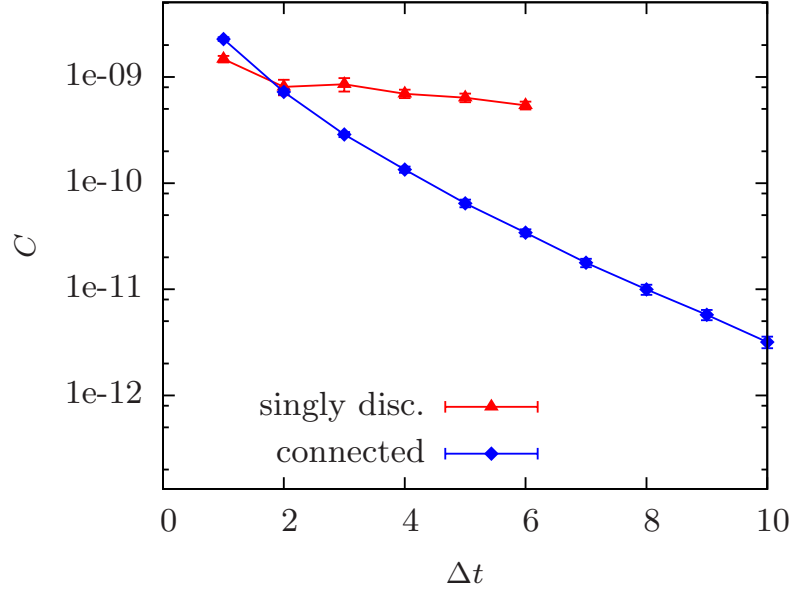


Figure 12: correlation function for the connected and the singly disconnected term of the four-quark correlator ($a_0(980)$ sector)

mass of 367 ± 145 MeV, which is not the mass we expect from the $a_0(980)$ meson (around 980 MeV). Due to the low statistic, the error is very large, but the value still suggests that there is an unexpected mixing with the pion (mass of the pion on given lattices is $m_\pi = 336$ MeV). This could be possible due to the parity breaking effect of the twisted mass action.

In order to observe possible mixing of the $a_0(980)$ four-quark and the pion, I will study the following transformations of the twisted mass action: Charge conjugation \mathcal{C} , parity \mathcal{P} , light isospin I_l and its third component, strange isospin I_s and its third component. Here, I_s is the equivalent of the light isospin for the strange doublet. The three components are given by the Pauli matrices $I_{s,j} = \tau^j(s)$ which only act on the strange doublet (s^+ , s^-)

In twisted mass, parity and isospin are no good quantum numbers anymore, so here I will focus on charge conjugation, the third component of both isospins, and the twisted mass parity which is $\mathcal{P} \circ I_{l,x} \circ I_{s,x}$. In Tab. 2 the continuum quantum numbers are for QCD with a degenerated strange doublet.

As one can see in Tab. 2 from the twisted mass quantum numbers pion and scalar meson cannot mix. However, pion and the four-quark operator I used can mix.

\mathcal{O}	continuum			twisted mass				
	I_l	I_s	\mathcal{P}	$I_{l,z}$	$I_{s,z}$	\mathcal{C}	\mathcal{P}^{tm}	$\mathcal{P}^{tm} \circ \mathcal{C}$
$\bar{d}\gamma_5 u$ (π)	1	0	−	1	0	xx	xx	−
$\bar{d}\mathbb{1}u$ (a_0)	1	0	+	1	0	xx	xx	+
$(\bar{d}\gamma_5 s^+)(\bar{s}^+ \gamma_5 u)$	1	xx	+	1	xx	xx	xx	xx
$(\bar{d}\gamma_5 s^+)(\bar{s}^+ \gamma_5 u) + (\bar{d}\gamma_5 s^-)(\bar{s}^- \gamma_5 u)$	1	0	+	1	0	xx	xx	+

Table 2: table of quantum numbers in the continuum and twisted mass for the pion, the $a_0(980)$ meson, the standard $a_0(980)$ four-quark operator and the improved one; xx means that the operator has no conserved quantum number

Using the second operator should prohibit a mixing with the pion. When using the symmetric operator

$$\mathcal{O}_S = (\bar{d}\gamma_5 s^+)(\bar{s}^+ \gamma_5 u) + (\bar{d}\gamma_5 s^-)(\bar{s}^- \gamma_5 u) \quad (6.1)$$

I obtain four singly disconnected graphs: $(s^+(t_0) s^+(t_1))$, $(s^+(t_0) s^-(t_1))$, $(s^-(t_0) s^+(t_1))$, $(s^-(t_0) s^-(t_1))$. Here, $(s^+(t_0) s^-(t_1))$ means that in the four-quark correlator there is a strange-plus loop at time t_0 and a strange-minus loop at time t_1 . When I go to QCD with one strange quark I obtain $4(s(t_0) s(t_1))$ which is the disconnected term of the continuum operator $O = (\bar{d}\gamma_5 s)(\bar{s}\gamma_5 u)$

When using the antisymmetric combination for the operator

$$\mathcal{O}_{AS} = (\bar{d}\gamma_5 s^+)(\bar{s}^+ \gamma_5 u) - (\bar{d}\gamma_5 s^-)(\bar{s}^- \gamma_5 u) \quad (6.2)$$

all disconnected terms will vanish in the continuum, because two of them will gain an additional minus sign and cancel the other two. Thus, this appears not to be a suitable operator.

7 Summary, Conclusion and Outlook

7.1 Summary & Conclusion

7.1.1 Meson study

The meson studies performed in this thesis were a preparative work for a larger spectroscopy project from the ETM collaboration. Here the spectrum of various strange and charmed mesons including gluonic excitations will be computed from $N_f = 2 + 1 + 1$ gauge field configurations. My work aimed at providing information about the effectiveness of several spectroscopy methods to this project.

I computed the noise-to-signal ratio for 24 different meson states. These 24 meson states in twisted mass correspond to 12 different meson states in the continuum. Three different methods were used to compute the appearing quark propagators. The most important findings are:

- For mesons the one-end trick is always better than the standard stochastic-source method.
- For light mesons and excited states, the one-end trick is slightly more effective than the point-source method.
- For heavy mesons both methods provide results of equal quality.

By using analytic model calculations I was able to show the advantage of the one-end trick over the standard stochastic-source method and showed how to estimate the increase of the noise-to-signal ratio over the temporal separation and presented two examples using lattice data. By studying the terms of the Dirac operator, I expected larger gauge noise, in comparison to the noise from the stochastic sources, for the light mesons and confirmed this with the numerical data. The numerical data also suggests a larger gauge noise for the scalar mesons.

I studied the influence of spin dilution on the noise-to-signal ratio. The numerical data suggests that, although using no spin dilution causes an increase of the noise-to-signal ratio for large temporal separations, the one-end trick without spin dilution should be preferred when applicable. I examined a smearing method, in which only one side of the propagator is smeared and compared the results to the standard method. I could not find an explicit advantage of only smearing the source or the

sink. Still, the one-sided methods, especially only smearing the sink, can be used to save computation time.

7.1.2 Four-quark study

The four-quark studies performed in this work are an additional study to a four-quark work of the ETM collaboration [26]. Because the disconnected terms were neglected in this work, my thesis aimed at providing preliminary information about the computation of singly disconnected diagrams, which can be included in future projects.

For the four-quark studies, I presented a comparison between two stochastic methods, which can be used to compute the singly disconnected diagram. My numerical data showed an advantage of the method where the noise is only located on one time slice and I was also able to analytically estimate the difference between the two methods.

Next, I computed the correlators of connected as well as singly disconnected terms of the D_{s0}^* and $a_0(980)$ four-quark candidates. The results suggest that the singly disconnected diagram can be computed without investing a large amount of computational cost. For the $a_0(980)$ candidate I studied the relation of the connected and singly-disconnected correlator and found an unexpected mixing with very light states.

In the last section I showed how the mixing could be avoided by using symmetries of the action in order to create a suitable four-quark operator.

7.2 Outlook

The lattices I used are rather small in comparison to recently used lattices ($32^3 \times 64$ or even larger). Furthermore, the analytic model suggests a \sqrt{V} dependence of the factor, by which the standard stochastic-source method and the one-end trick differ. Therefore, it would be interesting to extend my computations for different volumes and study the volume behavior of the results.

It would be interesting to find out how large the noise added by using the stochastic methods is in comparison to the gauge noise. This could be studied by computing the correlators for different numbers of samples of the stochastic sources. When

comparing the results of this study to the sample dependence of the noise-to-signal ratio suggested by the analytic model (N for standard stochastic-source method, \sqrt{N} for the one-end trick) the magnitude of which the stochastic noise contributes to the noise-to-signal ratio could possibly be estimated. Both of the mentioned studies are ongoing and will be presented in [22].

For the four-quark studies it would be helpful to investigate whether the operator introduced in the last section of my work will prevent a mixing of the possible four-quark states with light pseudo-scalar meson states.

In order to confirm or discard the existence of four-quark states, a very lengthy study is necessary. In a first step, a correlation matrix has to be constructed containing the complete four quark operator, the scalar meson and the two-meson state. After solving the generalized eigenvalue problem, one has to look for a third low-lying state. This possible study is very challenging to perform and will need a lot of computation time.

8 Bibliography

- [1] S. Godfrey and N. Isgur, “Mesons in a relativized quark model with chromodynamics,” *Phys. Rev. D* **32**, 189 (1985).
- [2] T. A. DeGrand, R. L. Jaffe, K. Johnson and J. E. Kiskis, “Masses and other parameters of the light hadrons,” *Phys. Rev. D* **12**, 2060 (1975).
- [3] H. Hamber, E. Marinari, G. Parisi and C. Rebbi, “Spectroscopy in a lattice gauge theory,” *Phys. Lett. B* **108**, 314 (1982).
- [4] A. M. Green *et al.* [UKQCD Collaboration], “Excited B mesons from the lattice,” *Phys. Rev. D* **69**, 094505 (2004) [hep-lat/0312007].
- [5] J. Beringer *et al.* (Particle Data Group), “Note on scalar mesons” PR D86, 010001 (2012) (URL: <http://pdg.lbl.gov>)
- [6] R. Baron *et al.* [ETM Collaboration], “Light meson physics from maximally twisted mass lattice QCD,” arXiv:0911.5061 [hep-lat].
- [7] B. Blossier *et al.* [ETM Collaboration], “Pseudoscalar decay constants of kaon and D-mesons from $N_f = 2$ twisted mass Lattice QCD,” *JHEP* **0907**, 043 (2009) [arXiv:0904.0954 [hep-lat]].
- [8] K. Jansen, C. Michael, A. Shindler and M. Wagner [ETM Collaboration], “The static-light meson spectrum from twisted mass lattice QCD,” *JHEP* **0812** (2008) 058 [arXiv:0810.1843 [hep-lat]].
- [9] C. Alexandrou *et al.* [European Twisted Mass Collaboration], “Light baryon masses with dynamical twisted mass fermions,” *Phys. Rev. D* **78** (2008) 014509 [arXiv:0803.3190 [hep-lat]].
- [10] D. Mohler and R. M. Woloshyn, “ D and D_s meson spectroscopy,” *Phys. Rev. D* **84**, 054505 (2011) [arXiv:1103.5506 [hep-lat]].
- [11] C. Alexandrou and G. Koutsou, “The static tetraquark and pentaquark potentials,” *Phys. Rev. D* **71**, 014504 (2005) [hep-lat/0407005].
- [12] S. Prelovsek, T. Draper, C. B. Lang, M. Limmer, K. -F. Liu, N. Mathur and D. Mohler, “Lattice study of light scalar tetraquarks with $I=0,2,1/2,3/2$: Are

σ and κ tetraquarks?,” Phys. Rev. D **82**, 094507 (2010) [arXiv:1005.0948 [hep-lat]].

- [13] E. Endress, A. Juttner and H. Wittig, “On the efficiency of stochastic volume sources for the determination of light meson masses,” arXiv:1111.5988 [hep-lat].
- [14] S. Bernardson, P. McCarty and C. Thron, “Monte Carlo methods for estimating linear combinations of inverse matrix entries in lattice QCD,” Comput. Phys. Commun. **78**, 256 (1993).
- [15] S. -J. Dong and K. -F. Liu, “Stochastic estimation with Z(2) noise,” Phys. Lett. B **328**, 130 (1994) [hep-lat/9308015].
- [16] M. Foster *et al.* [UKQCD Collaboration], “Quark mass dependence of hadron masses from lattice QCD,” Phys. Rev. D **59** (1999) 074503 [hep-lat/9810021].
- [17] C. McNeile *et al.* [UKQCD Collaboration], “Decay width of light quark hybrid meson from the lattice,” Phys. Rev. D **73** (2006) 074506 [hep-lat/0603007].
- [18] H. J. Rothe. *Lattice Gauge Theories: An Introduction*. World Scientific Pub Co Inc (4th edition), 2012.
- [19] M. Wagner, C. Wiese [ETM Collaboration], “The static-light baryon spectrum from twisted mass lattice QCD,” JHEP **1107** (2011) 016 [arXiv:1104.4921 [hep-lat]].
- [20] A. Shindler, “Twisted mass lattice QCD,” Phys. Rept. **461** (2008) 37 [arXiv:0707.4093 [hep-lat]].
- [21] B. Blossier, G. von Hippel, T. Mendes, R. Sommer and M. Della Morte, “Efficient use of the generalized eigenvalue problem,” PoS **LATTICE2008** (2008) 135 [arXiv:0808.1017 [hep-lat]].
- [22] C. Wiese, M. Wagner “The efficient computation of meson correlation functions,” in preparation.
- [23] A. Shindler, private communication.
- [24] C. Amsler and N. A. Tornqvist, “Mesons beyond the naive quark model,” Phys. Rept. **389**, 61 (2004).

- [25] C. McNeile, C. Michael and G. Thompson [UKQCD Collaboration], “Hadronic decay of a scalar B meson from the lattice,” Phys. Rev. D **70** (2004) 054501 [arXiv:hep-lat/0404010].
- [26] C. Alexandrou, J. Daldrop, M. Dalla Brida, M. Gravina, L. Scarzato, C. Urbach and M. Wagner [ETM Collaboration], “Lattice investigation of the tetraquark candidates $a_0(980)$ and κ ,” to be published.

Acknowledgments

First of all I would like to thank Marc Wagner for his great supervision of this thesis. This work was mostly done in his Emmy-Noether-Group "Lattice QCD with 2+1+1 dynamical quark flavors".

It is a pleasure to thank Andrea Shindler and Michael Müller-Preussker for helpful discussions.

The major part of computations has been performed at the PC farm at DESY Zeuthen. I thank DESY as well as its staff for technical advice and help.

I would like to thank the Konrad Zuse Zentrum für Informationstechnik Berlin as well as the Emmy-Noether-Programm of the DFG for financial support.

Finally, I acknowledge the emotional support by my parents and especially by Ann-Kathrin.

Selbstständigkeitserklärung

Hiermit versichere ich, dass ich die vorliegende Arbeit selbständig verfasst und keine anderen als die angegebenen Quellen und Hilfsmittel verwendet habe.

Berlin, den 24.09.2012

Christian Wiese